EPR Spectroscopy and Photophysics of the Lowest Photoactivated Triplet State of a Series of Highly Conjugated (Porphinato)Zn Arrays

P. J. Angiolillo,[†] Victor S.-Y. Lin,[‡] J. M. Vanderkooi,*[,†] and Michael J. Therien*[,‡]

Contribution from the Johnson Research Foundation, Department of Biochemistry and Biophysics, School of Medicine, University of Pennsylvania, Philadelphia, Pennsylvania 19104-6089, and Department of Chemistry, University of Pennsylvania, Philadelphia, Pennsylvania 19104-6323

Received July 3, 1995[⊗]

Abstract: The lowest photoexcited metastable triplet state of a family of highly conjugated (porphinato)zinc(II) arrays in which ethyne or butadiyne units bridge the macrocycle carbon frameworks, along with their ethyne- and butadiyne-elaborated monomeric porphyrinic building blocks, and parent (porphinato)zinc(II) precursor molecules were studied by electron paramagnetic resonance (EPR), transient triplet−triplet absorption, and phosphorescence emission. All EPR spectra of the excited monomeric precursors and dimeric and trimeric porphyrin arrays reflect symmetries of rhombic distortion ($|D| \geq 3|E|$) at 4 K and exhibit electron spin polarization patterns verifying that intersystem crossing from the first excited singlet state occurs predominantly through the $|T_z\rangle$ spin state sublevel. The zero field splitting (ZFS) parameters of the (porphinato)zinc monomers that bear ethynyl and butadiynyl groups as well as the conjugated porphyrin arrays are essentially temperature independent over a 4−100 K temperature range. This behavior is in contrast to the line shape changes typically seen in most monomeric closed-shell metalloporphyrin triplet states, signifying that the lowest excited triplet state possesses a symmetry lower than D_{4h} and hence not susceptible to Jahn−Teller instabilities. The magnitudes of the D values for all compounds except the *meso*-to-*meso* butadiyne-linked dimer lie in the range expected for monomeric (porphinato)zinc complexes, indicating that (1) there is no global delocalization of the triplet excitation and (2) the excitation can be considered to be localized on one of the monomeric subunits in the conjugated supramolecular chromophoric systems on the time scale probed by EPR. The type and mode of chromophore-to-chromophore connectivity does effect both spin distribution and spin alignment in the low temperature photoactivated triplet states of conjugated (porphinato)zinc arrays. For example, in the *meso*-to-*meso* butadiyne linked dimer, the $|D|$ value actually increases approximately 30% with respect to its monomeric precursor; this anomaly is interpreted as resulting from spin alignment in the molecular plane. A most striking feature is the persistence of electron spin polarization in most of the dimeric and trimeric porphyrin arrays under conditions of steady state illumination up to temperatures approaching the glass transition temperature ($T \approx 120$ K). Progressive power saturation experiments carried out on one of the dimeric porphyrin systems, in which an ethyne moiety bridges two (porphinato)zinc chromophores at their respective *meso*-carbon positions, reveals an exceptionally weak temperature dependence on the saturation parameter, $P_{1/2}$, along with no significant changes in either the ZFS parameters or line widths with increasing microwave power or temperature, indicating that spin lattice relaxation is long relative to de-excitation to the ground state over a broad temperature range. This anomalous effect is discussed from the standpoint of relaxation occurring primarily through matrix disorder modes.

Introduction

The past 5 years have seen the establishment of a new area of discovery research and promising technology—that of nanoscale molecular electronics.[1−6] Much of this development has been spurred by attempts to mimic or model the highly efficient electron and energy transfer processes typified by the reaction center and the associated light harvesting antenna complexes of green plants and photosynthetic organisms.

Although photoactivated triplet states of simple monomeric porphyrins and chlorophylls have served as probes for the study of energy and electron transfer in photosynthetic model systems,[7] multichromophoric assemblies play key roles in the biological photophysics of energy transduction. For example, the crystal structure of the bacterial reaction centers of *Rhodopseudomonas viridis*,[8−10] and *Rhodobacter sphaeroides* R-26[8,11] show that the bacteriochlorophyll molecules exist in a special dimeric arrangement; furthermore, the recently-reported structural study

[†] Johnson Research Foundation.

[‡] Department of Chemistry.

[⊗] Abstract published in *Advance ACS Abstracts*, November 15, 1995.

(1) Ashwell, G. J. In *Molecular Electronics*; Ashwell, G. J., Ed.; John Wiley and Sons, Inc.: New York, 1992.

(2) Kahn, O. *Molecular Magnetism*; VCH: New York, 1993.

(3) Miller, J. S. *Adv. Mater.* **1994**, *6*, 322−327.

(4) Benniston, A. C.; Goulle, V.; Harriman, A.; Lehn, J.-M.; Marczinke, B. *J. Chem. Phys.* **1994**, *98*, 7798−7804.

(5) Barigelletti, F.; Flamigni, L.; Balzani, V.; Collin, J. P.; Sauvage, J. P.; Sour, A.; Constable, E. C.; Thompson, A. M. W. C. *J. Am. Chem. Soc.* **1994**, *116*, 7692−7699.

(6) *Molecular and Biomolecular Electronics;* Advances in Chemistry Series 240; Birge, R. R., Ed.; American Chemical Society: Washington, D.C., 1994.

(7) Budil, D. E.; Thurnauer, M. C. *Biochim. Biophys. Acta* **1991**, *1057*, 1−41.

(8) Allen, J. P.; Feher, G.; Yeates, T. O.; Komiya, H.; Rees, D. C. *Proc. Natl. Acad. Sci. U.S.A.* **1987**, *84*, 5730−5734.

(9) Komiya, H.; Yeates, T. O.; Rees, D. C.; Allen, J. P.; Feher, G. *Proc. Natl. Acad. Sci. U.S.A.* **1988**, *85*, 9012−9016.

(10) Yeates, T. O.; Komiya, H.; Chirino, A.; Rees, D. C.; Allen, J. P.; Feher, G. *Proc. Natl. Acad. Sci. U.S.A.* **1988**, *85*, 7993−7997.

(11) Allen, J. P.; Feher, G.; Yeates, T. O.; Rees, D. C.; Deisenhofer, J.; Michel, H.; Huber, R. *Proc. Natl. Acad. Sci. U.S.A.* **1986**, *83*, 8589−8593.

0002-7863/95/1517-12514$09.00/0

of the antenna complex of *Rhodopseudomonas acidophila* highlights the importance of an organized constellation of bacteriochlorophyll *a* molecules in biological light harvesting and excitation transfer.[12] In such antenna systems, it has become clear that the electronic communication between the chromophores is both efficient and rapid. Key criteria for effective biomimetic modeling of such complex systems is predicated on the development of multipigment assemblies that not only have high oscillator strength absorption throughout the visible and high-energy near IR regions of the solar spectrum and significant overlap of their absorptive and emissive spectral bands but also possess precisely modulated interchromophore ground-state electronic and excitonic interactions.

Such interests have fueled the development of a variety of covalently linked multichromophoric systems, many of which are based on the porphyrin macrocycle. A variety of aromatic linkage motifs such as *o*-, *m*-, and *p*-phenylenes,[13-18] biphenyls,[18-20] naphthalenes,[21] anthracenes,[18,22] and diphenylacetylenes[23] as well as topological connectivities based on aliphatic[24] and vinylic[25] moieties have been utilized as organic scaffolding to bridge the chromophores in both dimeric and oligomeric porphyrin arrays.

For the most part, porphyrin arrays that feature a linear arrangement of chromophores bridged by aromatic units display relatively unspectacular interporphyrin electronic communication, as evinced by their optical spectra. This derives from the steric interactions between *ortho*-groups on the aromatic bridges with the porphyrin ring substituents. These interactions are substantial even when the aryl and porphyrinic substituents involved are hydrogen atoms, resulting in large dihedral angles between the arene and porphyrin ring systems, thus limiting the extent of π overlap between neighboring chromophores. Similar steric interactions diminish porphyrin−porphyrin electronic communication for the *trans*-vinyllic linkage topology, while aliphatic chromophore−chromophore bridges result in minimal interporphyrin electronic communication due to the poor coupling enabled by the bridge σ-symmetry orbitals. More substantial porphyrin−porphyrin electronic communication can be effected with aromatic, vinyllic, and aliphatic chromophore−chromophore bridges when they are engineered to hold the macrocycles rigidly in a face-to-face orientation at relatively small porphyrin−porphyrin interplanar separations;[26] while such molecules bear on the biomimetic chemistry of the special pair of bacteriochlorophyll b molecules of the photosynthetic reaction center, this spatial arrangement of chromophores appears not to be utilized in biological light harvesting and excitation transfer proteins.

Ethyne and butadiyne groups have been recently utilized as rigid molecular bridges in multiporphyrinic arrays to directly connect the carbon frameworks of the chromophores.[27-33] The optical properties of these arrays are not only distinct from those utilizing aryl-, vinyl-, or alkyl-type chromophore−chromophore connectivities; some of these supramolecular systems in fact feature porphyrin−porphyrin electronic interactions of unprecedented magnitude. We recently demonstrated that metal-mediated cross-coupling not only provides a straightforward entry into such highly-conjugated multichromophoric systems[31,34] but also enables considerable and predictable modulation of the supramolecular assembly's absorptive and emissive signatures, electrochemical properties, and excited-state anisotropy.[31-33] Such porphyrin arrays thus provide highly flexible model systems for probing fast and ultrafast electron and energy transfer events as well as a variety of excitation transfer processes relevant to the biological light harvesting antennae.

The zero field splitting (ZFS) parameters for triplet states have proven to be a sensitive indicator of triplet exciton dynamics in both molecular crystals and in conjugated molecules such as triptycene;[35] moreover, the triplet state electron paramagnetic resonance (EPR) spectra of monomeric and multimeric porphyrin systems have been of paramount importance in discerning the disposition of excitation energy.[36] In this study, we combine EPR spectroscopy, transient triplet-triplet absorption experiments, as well as phosphorescence emission studies to investigate the dynamics of the photoactivated metastable triplet states of a series of highly conjugated (porphinato)zinc(II) arrays, their associated ethyne-elaborated porphyrinic building blocks, and their parent (porphinato)zinc precursors.

Porphyrin Triplet Photophysics

The EPR Line Shape. The magnetic resonance of the lowest triplet excited state ($S = 1$) in porphyrins is that of a highly correlated spin system.[37,38] The spin Hamiltonian is governed mainly by the Zeeman interaction and the dipolar spin−spin

(12) McDermott, G.; Prince, S. M.; Freer, A. A.; Hawthornthwaite-Lawless, A. M.; Papiz, M. Z.; Cogdell, R. J.; Isaacs, N. W. *Nature (London)* **1995**, *374*, 517−521.
(13) Meier, H.; Kobuke, Y.; Kugimiya, S. *J. Chem. Soc., Chem. Commun.* **1989**, 923.
(14) Osuka, A.; Nakajima, S.; Nagata, T.; Muruyama, K.; Toriumi, K. *Angew. Chem., Int. Ed. Engl.* **1991**, *30*, 582−584.
(15) Tabushi, I.; Sasaki, T. *Tetrahedron Lett.* **1982**, 1913−1916.
(16) Sessler, J. L.; Hugdall, J.; Johnson, M. R. *J. Org. Chem.* **1986**, *51*, 2838−2840.
(17) Sessler, J. L.; Johnson, M. R.; Lin, T.-Y.; Creager, S. E. *J. Am. Chem. Soc.* **1988**, *110*, 3659−3661.
(18) Nagata, T.; Osuka, A.; Maruyama, K. *J. Am. Chem. Soc.* **1990**, *112*, 3054−3059.
(19) Helms, A.; Heiler, D.; McLendon, G. *J. Am. Chem. Soc.* **1991**, *113*, 4325−4327.
(20) Heiler, D.; McLendon, G.; Rogalskyj, P. *J. Am. Chem. Soc.* **1987**, *109*, 604−606.
(21) Osuka, A.; Maruyama, K. *J. Am. Chem. Soc.* **1988**, *110*, 4454−4456.
(22) Chang, C. K.; Abdalmuhdi, I. *J. Org. Chem.* **1983**, *48*, 5388−5390.
(23) Wagner, R. W.; Lindsey, J. S. *J. Am. Chem. Soc.* **1994**, *116*, 9759−9760.
(24) (a) Selensky, R.; Holten, D.; Windsor, M. W.; Paine, J. B., III; Dolphin, D. *Chem. Phys.* **1981**, *60*, 33−46. (b) Kamogawa, H.; Miyama, S.; Minoura, S. *Macromolecules* **1989**, *22*, 2123−2126. (c) Fleischer, E. B.; Shachter, A. M. *J. Heterocycl. Chem.* **1991**, *28*, 1693−1699. (d) Scamporrino, E.; Vitalini, D. *Macromolecules* **1992**, *25*, 1625−1632.
(25) Graça, M.; Vicente, H. Smith, K. M. *J. Org. Chem.* **1991**, *56*, 4407−4418.
(26) (a) Collman, J. P.; Anson, F. C.; Barnes, C. E.; Bencosme, C. S.; Geiger, T.; Evitt, E. R.; Kreh, R. P.; Meier, K.; Pettman, R. B. *J. Am. Chem. Soc.* **1983**, *105*, 2694−2699. (b) Chang, C. K.; Abdalmuhdi, I. *Agnew. Chem., Int. Ed. Engl.* **1984**, *23*, 164−165. (c) Eaton, S. S.; Eaton, G. R.; Chang, C. K. *J. Am. Chem. Soc.* **1985**, *107*, 3177−3184. (d) Hunter, C. A.; Sanders, J. K. M.; Stone, A. J. *Chem. Phys.* **1989**, *133*, 395−404. (e) Le Mest, Y., L'Her, M.; Hendricks, N. H.; Kim, K.; Collman, J. P. *Inorg. Chem.* **1992**, *31*, 835−847.
(27) Arnold, D. P.; Nitschinsk, L. J. *Tetrahedron* **1992**, *48*, 8781−8792.
(28) Arnold, D. P.; Nitschinsk, L. J. *Tetrahedron Lett.* **1993**, *34*, 693−696.
(29) Anderson, H. L.; Martin, S. J.; Bradley, D. D. C. *Angew. Chem., Int. Ed. Engl.* **1994**, *33*, 655−657.
(30) Anderson, H. L. *Inorg. Chem.* **1994**, *33*, 972−981.
(31) Lin, V. S.-Y.; DiMagno, S. G.; Therien, M. J. *Science (Washington, D. C.)* **1994**, *264*, 1105−1111.
(32) Lin, V. S.-Y.; Therien, M. J. *Chem. Eur. J.*, in press.
(33) Lin, V. S.-Y.; Therien, M. J. Manuscript in preparation
(34) (a) DiMagno, S. G.; Lin, V. S.-Y.; Therien, M. J. *J. Am. Chem. Soc.* **1993**, *115*, 2513−2515. (b) DiMagno, S. G.; Lin, V. S.-Y.; Therien, M. J. *J. Org. Chem.* **1993**, *58*, 5983−5993.
(35) Carrington, A.; McLachlan, A. D. *Introduction to Magnetic Resonance*; Chapman and Hall, 1967; pp 115−131, 204−220.
(36) (a) Ishii, K.; Yamauchi, S.; Ohba, Y.; Iwaizumi, M.; Uchiyama, I.; Hirota, N.; Maruyama, K.; Osuka, A. *J. Phys. Chem.* **1994**, *98*, 9431−9436. (b) Yamauchi, S.; Konami, H.; Akiyama, K.; Hatano, M.; Iwaizumi, M. *Mol. Phys.* **1994**, *83*, 335−344.
(37) Weltner, W. in *Magnetic Atoms and Molecules*; Dover Publications, Inc.: New York, 1983; pp 156−218.

interaction of the two electrons in the triplet molecular orbital. The nuclear hyperfine couplings are rarely, if at all, seen in randomly oriented triplets in external field, due to the large anisotropy. Within the molecular axis system, the total spin Hamiltonian describing the Zeeman interaction and the dipolar interaction between the two spins is

$$H_T = \beta_e \vec{H} \cdot \bar{\bar{g}} \cdot \vec{S} + \vec{S} \cdot \bar{\bar{D}} \cdot \vec{S} \quad (1)$$

Here $\vec{H}$ is applied magnetic field, $\vec{S}$ the total spin, $\bar{\bar{g}}$ the g-value tensor, and $\bar{\bar{D}}$ the zero field splitting tensor which contains contributions from the spin−spin dipolar and spin−orbit interactions. In the molecular axis system, selected to diagonalize the ZFS tensor, the Hamiltonian can be recast using two independent parameters, D and E, giving the familiar phenomenological spin Hamiltonian:

$$H_T = g_e \beta_e \vec{H} \cdot \vec{S} + D(S_z^2 - {}^1/_3 S^2) + E(S_x^2 - S_y^2) \quad (2)$$

The magnitude of the ZFS parameter, $|D|$, is a measure of the electronic spatial distribution of the triplet molecular orbital and is proportional to $\langle r^3 \rangle^{-1}$, and the magnitude ZFS parameter, $|E|$, is related to the degree of distortion from tetragonal symmetry. The quotient $3E/D$ lies in the range $-1 \leq 3E/D \leq 0$ where the two extremes represent axial symmetry ($E = 0$) and orthorhombic symmetry ($3|E|/|D| = 1$).[39]

The EPR line shape for randomly oriented triplets has been previously described.[40] The anisotropy of the zero field splittings, in general, leads to six observable lines or turning points in the first derivative spectrum. Assuming that D is positive, as is commonly observed for planar aromatics, and $E > 0$ (an arbitrary assignment) the $|0\rangle \leftrightarrow |+1\rangle$ transition has Z, X, and Y components at field positions displaced from that of free electron ($h\nu/g_e\beta_e$) by $-D$, $+(D - 3E)/2$, and $+(D + 3E)/2$, corresponding to Z_I, X_I, and Y_I field positions, respectively. Likewise, the $|0\rangle \leftrightarrow |-1\rangle$ transition has lines at field positions displaced from g_e by $+D$, $-(D - 3E)/2$, and $-(D + 3E)/2$ that are defined as the Z_{II}, X_{II}, and Y_{II} transitions, respectively, following the convention of Thurnauer.[41] Thus, from the resulting randomly oriented spectrum, ZFS parameters are readily extractable, with the separations in field units between pairs of transitions defined as $\Delta H_z = 2|D|$, $\Delta H_y = |D| + 3|E|$, and $\Delta H_x = |D| - 3|E|$.

Electron Spin Polarization and Spin Lattice Relaxation. Spin state dynamics can be obtained from the EPR excited triplet spectrum under steady state illumination conditions.[42,43] Entry into the lowest triplet state is governed primarily by spin−orbit coupling. Consequently, at temperatures (typically in the vicinity of liquid helium) where the $S_0 \leftarrow T_1$ lifetime is short compared to the spin lattice relaxation time between two spin state sublevels (T_1), a non-Boltzmann occupation (electron spin polarization or, more appropriately, electron spin alignment) of the triplet manifold results. Hence, some transitions will be emissive (e) in nature while those that are absorptive (a) will be enhanced. The resulting polarization pattern of absorptions and emissions under conditions of steady state illumination can thus be used to ascertain information concerning ISC, spin dynamics, and relaxation.[44]

Dynamic Jahn−Teller Effect. For square planar metalloporphyrins, the lowest triplet should be spatially degenerate in the D_{4h} point group and have a representation of ^3E_u.[45] Since a porphyrin with a C_4 or S_4 symmetry element is Jahn−Teller (JT) unstable, it is subject to symmetry-relieving interactions that result in two energy equivalent triplet states.[46] Jahn−Teller instability alone is not enough to relieve the energy degeneracy of the triplet state, but interactions with axial ligands, porphyrin substituents, or local environment (solvent, protein) may stabilize one state relative to the other by an energy of δ_{JT}. The resulting EPR spectrum, when $\delta_{JT} \gg k_B T$, will show a static distortion with a non-zero $|E|$, with a splitting between the X and Y transitions (ΔH_{xy}) equal to $3|E|$. However, at temperatures that are comparable to or exceed the JT splitting energy, the X and Y transitions will merge, with complete coalescence occurring when both states are equally populated and when the exchange frequency, ω_{JT}, is greater than the separation of the X and Y transitions ($\omega_{JT} \gg g_e\beta_e\Delta H_{xy}$).[35,46] This temperature dependence of the X and Y transitions has been termed the "dynamic Jahn−Teller effect". Systems which manifest this phenomenon will exhibit low temperature EPR spectra with a rhombic line shape and with increasing temperature will evolve into a spectrum demonstrating axial symmetry ($E \approx 0$).

The predominate theory to account for the dynamic JT effect involves coupling of the triplet state to one of the in-plane porphyrin vibrational modes, giving rise to two vibronic triplets separated in energy by δ_{JT}.[45,47] For square planar porphyrins with D_{4h} symmetry, coupling to either b_{1g} or b_{2g} vibrational modes has the effect of merely changing the sign of E but not its absolute value. The distortions are equivalent to an interchange of the x and y molecular axes. The ramification is that as $k_B T \gg \delta_{JT}$, the E value should approach zero and a coalescence of the Y and X canonical transitions should occur.

Experimental Section

Materials. All manipulations were carried out under nitrogen previously passed through an O_2 scrubbing tower (Schweizerhall R3−11 catalyst) and a drying tower (Linde 3-Å molecular sieves) unless otherwise stated. Air-sensitive solids were handled in a Braun 150-M glovebox. Standard Schlenk techniques were employed to manipulate air-sensitive solutions. All solvents utilized in this work were obtained from Fisher Scientific (HPLC Grade). 2-Methyltetrahydrofuran (2MTHF) and toluene were predried over 4 Å molecular sieves and then distilled from Na/benzophenone under N_2. Pyridine was distilled under N_2 from barium oxide.

Monomeric, Dimeric, and Trimeric (Porphinato)zinc Complexes. (5,15-Diphenylporphinato)zinc(II) (**1**) and (5,10,15,20-tetraphenylporphinato)zinc(II) (**5**) were prepared by traditional porphyrin synthetic methods.[34,48] [5-[(Trimethylsilyl)ethynyl]-10,20-diphenylporphinato]-zinc(II) (**2**), [5,15-bis[(trimethysilyl)ethynyl]-10,20-diphenylporphinato]-zinc(II) (**3**), [5,15-bis(trimethysilylbutadiynyl)-10,20-diphenylporphinato]-zinc(II) (**4**), [2-ethynyl-5,10,15,20-tetraphenylporphinato]zinc(II) (**6**), [2,12-diethynyl-5,10,15,20-tetraphenylporphinato]zinc(II) (**7**), 5,5′-bis-[(10,20-diphenylporphinato)zincio(II)]ethyne (**8**), 5,5′-bis[(10,20-diphenylporphinato)zincio(II)]butadiyne (**9**), 5,15-bis{5,5′-[(10,20-diphe-

(38) Slichter, C. P. *Principles of Magnetic Resonance*, 3rd ed.; Springer-Verlag: New York, 1990; pp 89−92.
(39) Poole, C. P.; Farach, H. A.; Jackson, W. K. *J. Chem. Phys.* **1974**, *61*, 2220−2221.
(40) (a) Wasserman, E.; Snyder, L. C.; Yager, W. A. *J. Chem. Phys.* **1964**, *41*, 1763−1772. (b) Kottis, P.; Lefrebvre, R. *J. Chem. Phys.* **1964**, *41*, 379−393.
(41) Thurnauer, M. C. *Rev. Chem. Intermed.* **1979**, *3*, 197−230.
(42) Thurnauer, M. C.; Katz, J. J.; Norris, J. R. *Proc. Natl. Acad. Sci. U.S.A.* **1975**, *72*, 3270−3274.
(43) McGlynn, S. P.; Azumi, T.; Kinoshita, M. *Spectroscopy of the Triplet State*; Prentice Hall: Englewood Cliffs, NJ, 1969.
(44) Hausser, K. H.; Wolf, H. C. In *Optical Spin Polarization in Molecular Crystals*; Waugh, J. S., Ed.; 1976; pp 85−121.
(45) van der Waals, J. H.; van Dorp, W. G.; Schaafsma, T. J. In *The Porphyrins*; Dolphin, D., Ed.; Academic Press: London, 1978; Vol. III, pp 257−312.
(46) Hoffman, B. M.; Ratner, M. A. *Mol. Phys.* **1978**, *35*, 901−925.
(47) (a) De Groot, M. S.; Hesselmann, I. A.; Van der Waals, J. H. *Mol. Phys.* **1969**, *1*, 61−68. (b) Sherz, A. N.; Levanaon, H. *J. Phys. Chem.* **1980**, *84*, 324−336.
(48) Kim, J. B.; Adler, A. D.; Longo, F. R. In *The Porphyrins*; Dolphin, D., Ed.; Academic Press: London, 1978; Vol. I.

nylporphinato)zincio(II)]ethynyl}(10,20-diphenylporphinato)zinc(II) (**10**), 2,2′-bis[(5,10,15,20-tetraphenylporphinato)zincio(II)]ethyne (**11**), 2,2′-bis[(5,10,15,20-tetraphenylporphinato)zincio(II)]butadiyne (**12**), 2,12-bis{2,2′-[(5′,10′,15′,20′-tetraphenylporphinato)zincio(II)]butadiynyl}-(5,10,15,20-tetraphenylporphinato)zinc(II) (**13**), 2-[(5,10,15,20-tetraphenylporphinato)zincio(II)]-5′-[10′,20′-diphenylporphinato)zincio(II)]-ethyne (**14**), and 2-[(5,10,15,20-tetraphenylporphinato)zinc(II)]-[5′,-10′,-20′-diphenylporphinato)zincio(II)]butadiyne (**15**) were synthesized using metal-mediated cross-coupling methodologies reported previously.[31,32,34]

EPR Spectroscopy. Electron paramagnetic resonance experiments were performed with a Bruker ESP 300E spectrometer. Intracavity illumination was performed directly through the front louvers with fiber optics (Eska, Mitsubishi Corp.) using a 150 W Kuda quartz−halogen illuminator with appropriate filtration for infrared radiation (Corning blue heat filter or 1 M $CuSO_4$). Temperatures were maintained utilizing an Oxford ESR 900 continuous flow liquid helium cryostat controlled with an Oxford ITC4 temperature controller. Frequency was measured with a Hewlett-Packard 5350B microwave frequency counter. All experiments (except for saturation profiles) were conducted at microwave powers that ensured there were no saturation of resonances. Progressive power saturation profiles were obtained automatically on the ESP 300 by following the low-field Z canonical transition as a function of input microwave power. Microwave power was read directly from the bridge-controller file. After each microwave power saturation profile at an elevated temperature, the temperature was returned to 4 K and spectra were recorded to check for any degradation of porphyrin after prolonged irradiation. No changes in ZFS or spectral line shape were evident after each power saturation study performed. Data were analyzed and fit according to methods described by Portis[49] and Castner.[50]

Transient Optical Spectra. Transient absorption spectra of excited state species were obtained at the Regional Laser and Biotechnology Laboratory at the University of Pennsylvania on an instrument described in detail previously.[51] The compounds were excited into the lowest triplet state via the first excited singlet state with 350 nm radiation obtained from a Q-switched Nd:Yag laser with a repetition rate of 10 Hz (1−5 mJ). The pump−probe delay times were varied from 1 ns to the instrumental limit of approximately 10 ms with a Princeton Research digital delay generator. All solutions were prepared in dry, degassed 1:10 pyridine:toluene and adjusted in concentration to give 0.2−0.4 OD absorption.

Emission Spectra. Phosphorescence emission spectra of compounds **1**−**15** were obtained at 77 K in glassy 2 MTHF matrices utilizing a SPEX UV/Vis/NIR spectrophotometry system.

Results

I. Zero Field Splitting Parameters and Symmetry Considerations. Monomers. Figures 1 and 2 show the EPR spectra of the $|\Delta M_s| = 1$ region of the photoactivated triplet state of the parent monomers and their acetylenic derivatives that were utilized in the construction of the dimeric and trimeric (porphinato)zinc arrays. Since in most cases the transitions were well-separated, the $|D|$ and $|E|$ ZFS parameters were determined directly from the EPR spectrum;[39] these values, in addition to the calculated asymmetry parameter $3|E|/|D|$, are listed in Table 1. As is evident, all compounds exhibit electron spin polarization at 4 K. The polarization patterns of **a-a e-e** for **1**, **5**, **6**, and **7** and **aaa eee** for **2**, **3**, and **4** indicate that intersystem crossing (ISC) from the first excited singlet state occurs predominantly through the $|T_z\rangle$ spin state sublevel and partially into the $|T_x\rangle$ spin state sublevel for **1**, **5**, **6**, and **7**. $|\Delta M_s| = 2$ absorptive transitions at $g = 4.00$ were observed for all monomeric compounds at 4 K, though due to the non-Boltzmann occupation of the triplet manifold at this temperature it was significantly weaker than the transitions in the $|\Delta M_s| = 1$ region

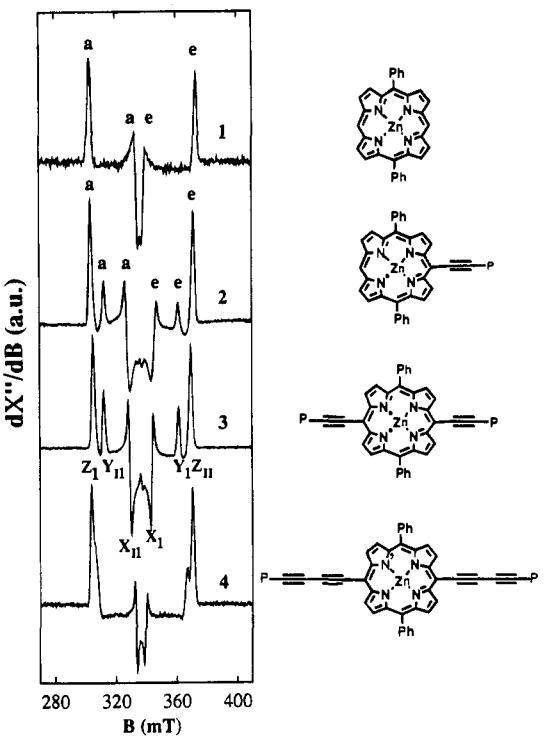

Figure 1. Photoactivated triplet state EPR spectra of ZnDPP and a series of its *meso*-ethynyl and -butadiynyl elaborated derivatives in the $|\Delta M_s| = 1$ region. All (porphinato)zinc concentrations were approximately 1 mM in a 1:10 pyridine:toluene glassy matrix. All spectra were recorded at 4 K, with a 2.0 mT modulation amplitude (100 kHz) and a microwave power of 2 μW. Absorption and emission peaks have been labeled **a** and **e**, respectively; canonical directions are as indicated following the convention outlined in the Introduction. P indicates that the ethyne or butadiyne group bears a trimethylsilyl protecting group.

(data not shown). Covalent attachment of ethynyl groups to the porphyrin periphery slightly reduces the $|D|$ ZFS parameters, indicating increased electron delocalization. Note that the attachment of an acetylenyl moiety to the porphyrin *meso* position significantly affects the $|E|$ ZFS parameter of **2**, reducing it to approximately 50% of the value observed for its precursor molecule **1** at low temperatures. This effect is not as pronounced for either the 2-ethynyl (**6**) or 2,12-diethynyl (**7**) derivatives of ZnTPP (**5**). Increasing conjugation in monomers **2**−**4**, in which one ethynyl, two ethynyl, and two butadiynyl groups are respectively attached to the *meso* porphyrin positions, correlates with a concomitantly increasing $|E|$ ZFS parameter. Similar attachment of ethynyl moieties porphyrin to the β position (molecules **6** and **7**) resulted in no significant change in either the $|D|$ or $|E|$ ZFS parameters (Table 1).

The temperature dependence of the photoactivated triplet state was examined for compounds **1**−**7**; ZnDPP (**1**) (Figure 3A) and ZnTPP (**5**) (not shown) show temperature dependent line shapes that have been interpreted in terms of the dynamic Jahn−Teller effect.[47,52] Such spectra are observed for orbitally degenerate triplets and therefore indicate that the triplet molecular orbitals of both these species are D_{4h} symmetry by the criteria of EPR; such a result is consistent with the fact that steric interactions significantly reduce the potential conjugative interactions between the aryl and porphyryl aromatic ring systems, with the result that the porphyrin frontier orbitals remain relatively unperturbed. **1** and **5** both evolve into triplet EPR spectral line shapes demonstrating axial symmetry ($E \sim 0$); the temperature at which coalescence is first seen is higher in **5** (80 K) than in

(49) Portis, A. M. *Phys. Rev.* **1953**, *91*, 1071−1078.
(50) Castner, T. G. *Phys. Rev. 115*, 1506−1515.
(51) Papp, S.; Vanderkooi, J. M.; Owen, C. S.; Holtom, G. R.; Phillips, C. M. *Biophys. J.* **1990**, *58*, 177−186.
(52) Angiolillo, P. J.; Vanderkooi, J. M. *Biophys. J.* **1995**, *68*, 2505−2518.

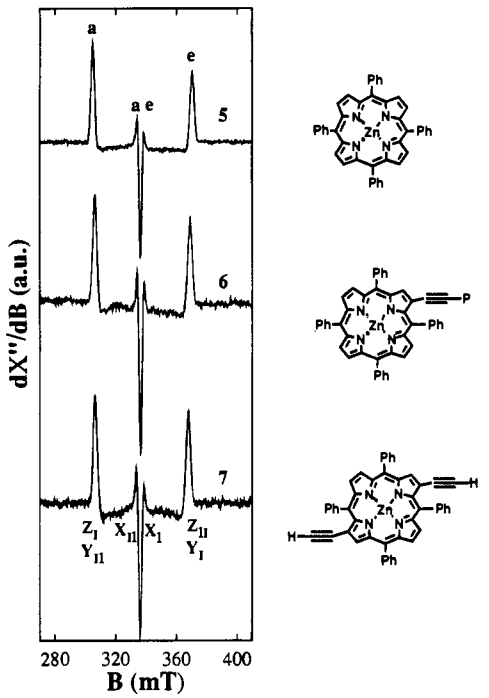

Figure 2. Photoactivated triplet state EPR spectra of ZnTPP and two of its β-ethynyl-elaborated derivatives in the $|\Delta M_s| = 1$ region. All (porphinato)zinc concentrations approximately 1 mM in a 1:10 pyridine: toluene glassy matrix. All spectra were recorded at 4 K, with a 2.0 mT modulation amplitude (100 kHz) and a microwave power of 2 μW. Absorption and emission peaks have been labeled **a** and **e**, respectively; canonical directions are as indicated following the convention outlined in the Introduction. P indicates that the ethyne group bears a trimethylsilyl protecting group.

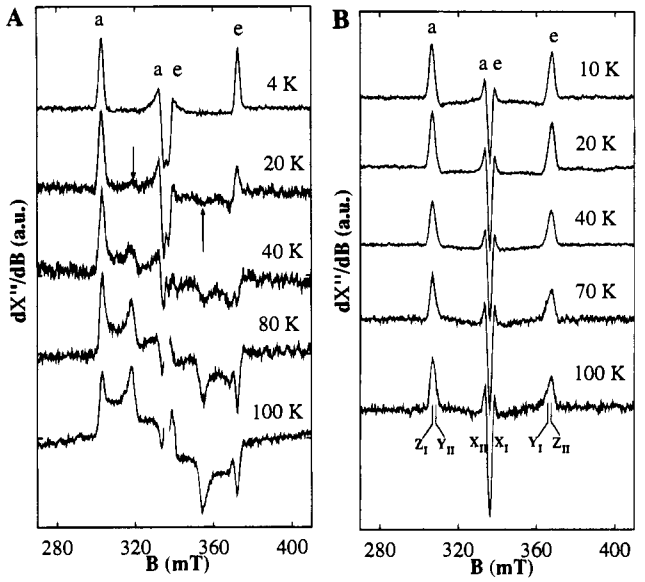

Figure 3. Temperature dependent triplet EPR spectra of monomeric (porphinato)zinc complexes **1** and **7**. EPR conditions are as specified in Figure 1 except for microwave powers which are as follows: (A) compound **1**: 4 K, 2 μW; 20 K, 50 μW; 40 K, 500 μW; 80 K 10 μW; 100 K, 50 μW. (B) Compound **7**: 10 K, 2 μW; 20 K, 10 μW; 40 K, 10 μW; 70 K, 50 μW; 100 K, 50 μW.

1 (20 K), indicating that the δ_{JT} is larger in **5**. Temperature dependent line shapes reflecting dynamic events were not seen for any of the porphyrin monomers bearing ethynyl or butadiynyl groups (molecules **2**, **3**, **4**, **6**, and **7**) over the 4−90 K temperature domain. Figure 3B displays the temperature dependent EPR data for compound **7**.

***Meso*-to-*Meso* Ethynyl- and Butadiynyl-Linked Porphyrin Arrays.** The EPR spectra ($|\Delta M_s| = 1$ region) recorded at 4 K of the lowest excited triplet state of the porphyrin arrays that feature *meso*-to-*meso* ethyne or butadiyne bridges fusing ZnDPP monomer units are given in Figure 4. All three compounds exhibit spin polarization with patterns signifying that ISC is dominated by entry into the $|T_z\rangle$ spin state sublevel. For the *meso*-to-*meso* ethynyl-bridged dimer (**8**), the line shape starkly contrasts that of **1** and its *meso*-acetylenyl derivative, 5-ethynyl-ZnDPP (**2**). The 4 K photoactivated triplet EPR spectrum of the *meso*-to-*meso* butadiyne-bridged dimer, **9**, differs remarkably from **8**. Compound **9**'s spectrum is a composite of two distinct triplet states possessing $|E|$ values of 0.0097 and 0.0092 cm^{-1}, corresponding respectively to the major and minor signals. Ever more striking is the observation that the $|D|$ value is larger than those typical of monomeric (porphinato)zinc complexes. The tris[(porphinato)zinc] complex (**10**), which features two ethyne moieties connecting the three [5,15-diphenylporphinato]zinc macrocycles at their respective *meso*-carbon positions, demon-

Table 1. Observed ZFS Parameters of the Monomeric, Dimeric, and Trimeric (Porphinato)zinc Complexes

	compd	solvent[a]	T (K)	$\lvert D\rvert$[b] (cm^{-1})	$\lvert E\rvert$[b] (cm^{-1})	$3\lvert E\rvert/\lvert D\rvert$
1	ZnDPP	pyr:tol	4−30	0.0326	0.0094	0.865
1	ZnDPP	pyr:tol	> 30	0.0326	~0[c]	
2	5-ethynyl-ZnDPP	pyr:tol	4−70	0.0315	0.0048	0.457
3	5,15-diethynyl-ZnDPP	pyr:tol	4−70	0.0301	0.0053	0.528
4	5,15-butadiynyl-ZnDPP	pyr:tol	4−70	0.0309	0.0084	0.816
5	ZnTPP	pyr:tol	4	0.0306	0.0095	0.931
5	ZnTPP	pyr:tol	>80	0.0303	~0[c]	
6	2-ethynyl-ZnTPP	pyr:tol	4	0.0292	0.0092	0.951
7	2,12-diethynyl-ZnTPP	pyr:tol	4−90	0.0285	0.0087	0.911
8	*meso*-to-*meso* ethyne-briged dimer	pyr:tol	4−100	0.0319	NR	
8	*meso*-to-*meso* ethyne-briged dimer	2MTHF	4−100	0.0323	NR	
9	*meso*-to-*meso* butadiyne-bridged dimer	pyr:tol	4	0.0447	0.0097	0.65
					0.0092	0.65
10	*meso*-to-*meso* ethyne-bridged trimer	2MTHF	4	0.0303	NR	
11	β-to-β ethyne-bridged dimer	pyr:tol	4	0.0281	0.0085	0.906
12	β-to-β butadiyne-bridged dimer	pyr:tol	4	0.0286	0.0086	0.900
13	β-to-β butadiyne-bridged trimer	pyr:tol	4	0.0279	0.0083	0.891
14	*meso*-to-β ethyne-bridged dimer	pyr:tol	4−70	0.0283	0.0083	0.879
				0.0313	NR	
15	*meso*-to-β butadiyne-bridged dimer	pyr:tol	4	0.0351	0.0105	0.897

[a] pyr:tol = 1:10 pyridine:toluene; 2MTHF = 2-methyltetrahydrofuran (neat). NR = value undetermined since distinct resonances were not observed. [b] ZFS values ± 0.0002 cm^{-1} for D and ± 0.0002 cm^{-1} for E. [c] Indicates the emergence of an axially symmetric signal ($E \approx 0$) in addition to the nonaxial component seen at low temperature.

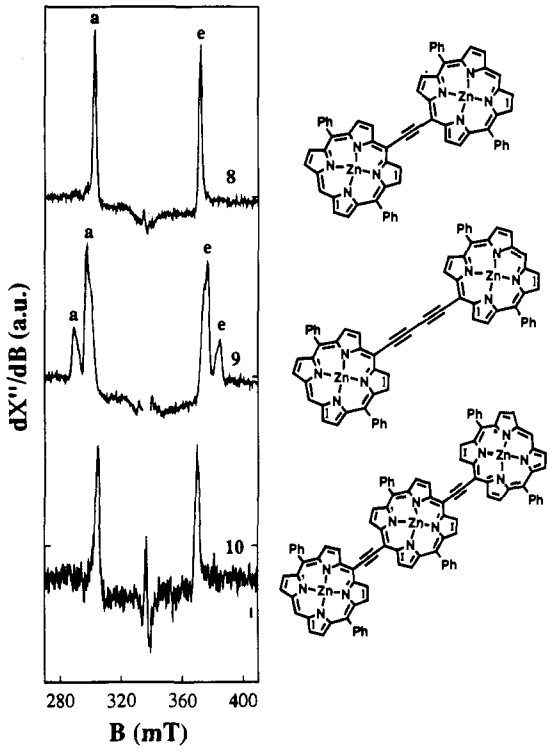

Figure 4. EPR spectra of the photoactivated triplet state of the *meso*-to-*meso* ethyne- and butadiyne-bridged dimeric and trimeric (porphinato)zinc arrays: (A) *meso*-to-*meso* ethyne-bridged dimer **8**, in 1:10 pyridine:toluene; (B) *meso*-to-*meso* butadiyne-bridged dimer **9**, in 1:10 pyridine:toluene; (C) *meso*-to-*meso* ethyne-bridged trimer **10**, in 2 MTHF. Chromophore concentrations were approximately 1 mM except for **10**, which was 0.25 mM due to its lower solubility. Experimental conditions: temperature = 4 K; modulation amplitude = 2.0 mT at 100 kHz; microwave power = 2 μW.

strates a line shape not unlike that of **8**, except that the $|D|$ ZFS parameter is slightly smaller in magnitude (Table 1).

EPR spectral temperature-dependence studies for compounds **8** and **9** are shown in Figure 5A and B, respectively. Over a 4−70 K temperature range, compound **8** maintains electron spin polarization, the intensity of which is reduced only by a factor of 3 as the temperature is raised from 30 to 70 K, indicating that there is little temperature dependence of the spin lattice relaxation time. Furthermore, no change in line shape is evident in this experiment for compound **8**. Compound **9** demonstrates similarly little thermalization over this temperature domain as can be seen in Figure 5B; however, the signal due to the photoactivated triplet species that corresponds to the larger $|E|$ value ($|E| = 0.0092$ cm^{-1}) vanishes by 70 K.

As a consequence of the nonthermalization of the line shape with respect to temperature evinced in the *meso*-to-*meso* ethyne-bridged dimer (**8**), temperature-dependent microwave power saturation measurements were performed between 4 and 50 K. The line width of the Z_I and Z_{II} transitions remain constant over the temperature range studied, indicating no significant change in the spin−spin relaxation time (T_2). The microwave power saturation measurements shown in Figure 6 demonstrate that the power saturation parameter, $P_{1/2}$ (a measure of $1/T_1T_2$), depends weakly on temperature with an apparent quadratic dependence on that parameter over the 4−50 K range (Figure 6, inset).

***β*-to-*β* Ethynyl- and Butadiynyl-Linked Porphyrin Arrays.** Figure 7 shows the $|\Delta M_s| = 1$ region of the lowest photoactivated triplet state of porphyrin arrays that feature *β*-to-*β* ethyne- or butadiyne-bridges that connect ZnTPP monomeric units. The ethyne- and butadiyne-linked dimers (**11** and **12**) as well as the

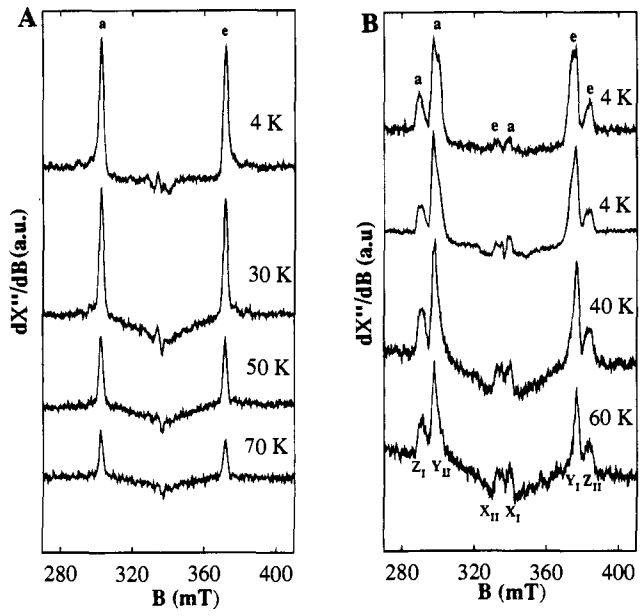

Figure 5. Temperature dependent triplet EPR spectra of *meso*-to-*meso* ethyne- and butadiyne-bridged dimeric (porphinato)zinc arrays **8** and **9**. EPR conditions as given in Figure 4 except for microwave powers which are as follows: (A) Compound **8**: 4K, 2 μW; 30 K, 50 K; 70 K, 30 μW. *Temperatures are indicated on the figure.* (B) Compound **9**: 4K, 2 μW; 4K, 100 μW; 40K, 100 μW; 60K, 100 μW. Temperatures are indicated on the figure.

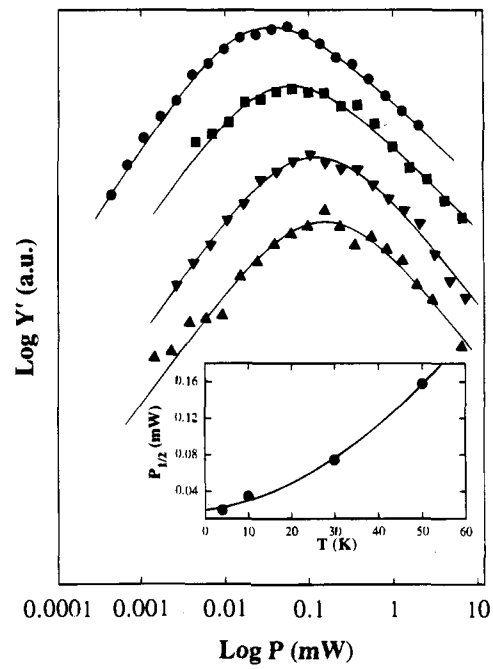

Figure 6. Intensity of low-field Z canonical transitions as a function of incident microwave power for compound **8**. Y' is the peak intensity of the low field Z canonical transition (Z_I). The solid lines are a fit to $Y' = A\sqrt{P}/(1 + P/P_{1/2})^{b/2}$, where P is the incident microwave power, $P_{1/2}$ is the saturation parameter, A is an instrumental constant, and b is a measure of inhomogeneity (as described in the text). Temperatures are indicated by the following symbols: circles, 4 K; squares, 10 K; inverted triangles, 30 K; triangles, 50 K. Inset plots $P_{1/2}$ as a function of temperature. The solid line is a least squares fit to $P_{1/2} = AT^2 + C$ ($A = 0.054$, $C = 24.33$). Experimental conditions are the same as that described in Figure 4; the $P_{1/2}$ values are as follows: 4 K, 20 ± 1.3 μW; 10 K, 34 ± 4 μW; 30 K, 74 ± 6 μW; 50 K, 157 ± 24 μW.

trimer (**13**) that features two butadiyne moieties fusing two (tetraphenylporphinato)zinc chromophores to a central ZnTPP unit at its 2- and 12-positions exhibit line shapes remarkably

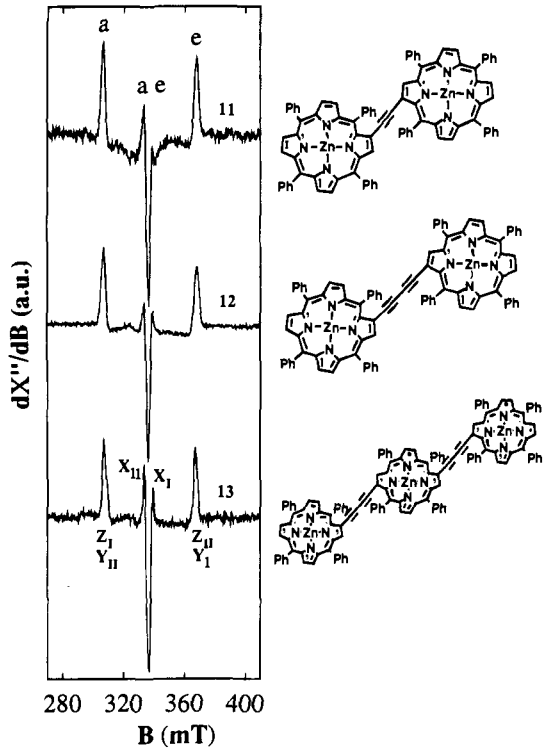

Figure 7. Photoactivated triplet EPR spectra of the β- to-β ethyne- and butadiyne-bridged (porphinato)zinc arrays: (A) β-to-β ethyne-bridged dimer **11**; (B) β-to-β butadiyne-bridged dimer **12**; (C) β-to-β butadiyne-bridged trimer **13**. Concentrations of the (porphinato)zinc arrays were approximately 1 mM in a 1:10 pyridine:toluene glassy matrix. Experimental conditions: temperature = 4 K; modulation amplitude = 2.0 mT at 100 kHz; microwave power = 2 μW.

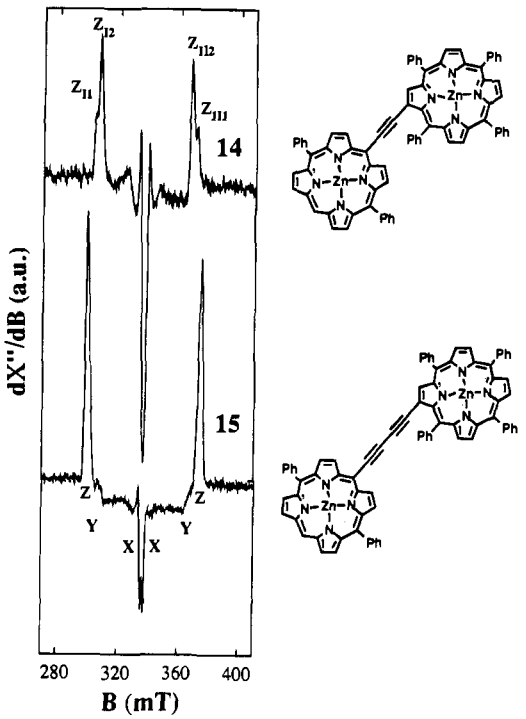

Figure 8. EPR spectra of the photoactivated triplet state of the *meso*-to-β ethyne- and butadiyne-bridged (porphinato)zinc arrays. (A) *meso*-to-β ethyne-bridged dimer **14**; (B) *meso*-to-β butadiyne-bridged dimer **15**. All chromophore concentrations are approximately 1 mM in 1:10 pyridine:toluene glassy matrices. Experimental conditions: temperature = 4 K; modulation amplitude = 2.0 mT at 100 kHz; microwave power = 2 μW.

similar to the parent monomeric compound ZnTPP (Figure 2). All three compounds at 4 K have a spin polarization pattern of **a-a e-e** indicating that the $|T_z\rangle$ spin state sublevel provides the predominant path into the triplet manifold from the first excited singlet state, as was seen in the porphyrin arrays that feature the *meso*-to-*meso* linkage topology. The $|D|$ ZFS parameters for **6** and **7** are only slightly smaller relative to that for the parent monomeric unit ZnTPP (Table 1), while compounds **11**−**13** all exhibit an approximate 10% reduction in this parameter.

***Meso*-to-β Ethynyl- and Butadiynyl-Linked Porphyrin Arrays.** Figure 8 shows the $|\Delta M_s| = 1$ region of the lowest photoactivated triplet state of the meso-to-β ethyne- and butadiyne-bridged ZnDPP−ZnTPP heterodimers. Compounds **14** and **15** have a spin polarization pattern of **a-a e-e** at 4 K, consistent with the theme that the $|T_z\rangle$ spin state sublevel establishes the dominant pathway into the triplet manifold from the first excited singlet state for these conjugated, multichromophoric porphyrin arrays. The EPR spectrum of **14** shows clearly two pairs of Z transitions. The higher intensity pair of Z transitions gives a $|D|$ value of 0.0283 cm^{-1}, while the pair of transitions defined by the distinct shoulders to the low and high field sides of the major absorptions define a triplet state with a $|D|$ value of 0.0313 cm^{-1}. The temperature-dependent EPR spectra of **14** reveal that the outer transitions decay by 50 K (Figure 9). The EPR spectrum of the photoactivated triplet state of compound **15**, which features a butadiyne bridge between ZnTPP and ZnDPP, demonstrates a slightly larger $|D|$ value than is expected given the minor change in molecular length between heterodimers **14** and **15**.

II. Transient T−T Absorption and Phosphorescence Emission. To further characterize the nature of the triplet excited states of these compounds, transient triplet−triplet ($T_1 \rightarrow T_n$) absorption and phosphorescence emission measurements were performed as well. Representative transient absorption spectra at room temperature are shown in Figure 10 for *meso*-to-*meso* ethyne-bridged arrays **8** and **10**. The spectra are characterized by a bleach in the Soret region and an increase in

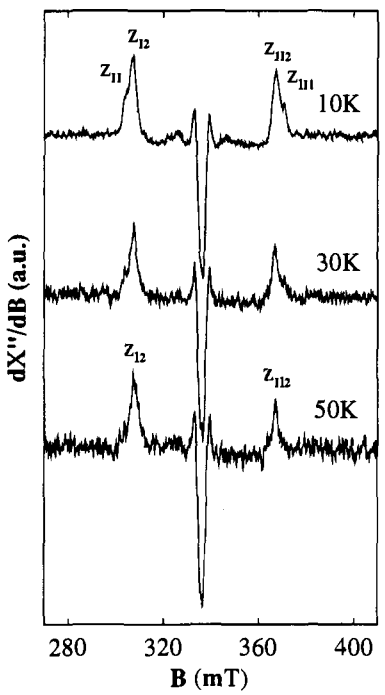

Figure 9. Temperature dependence of the photoactivated triplet EPR spectrum of compound **14**. Experimental conditions: modulation amplitude, 2.0 mT (100 kHz); microwave power 10 K, 20 μW; 30 K, 50 μW; 50 K, 100 μW. Temperatures are indicated on the figure.

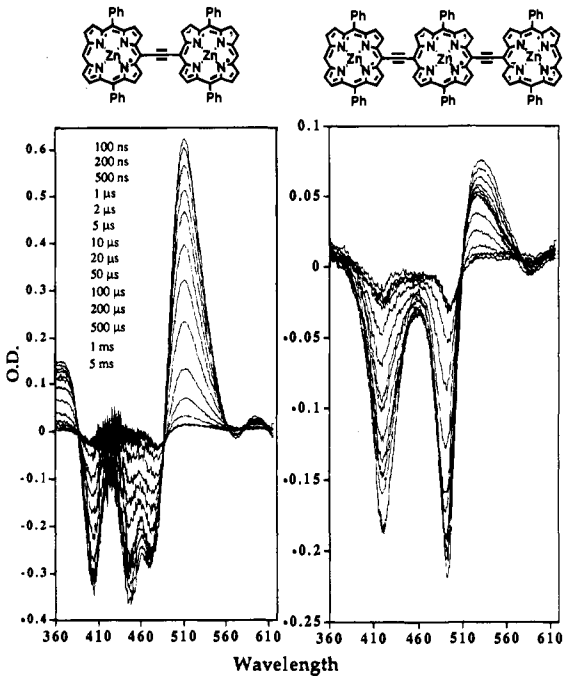

Figure 10. Transient triplet−triplet absorption spectra of compounds **8** and **9**. Experimental conditions: temperature = 25 °C; λ_{ex} = 350 nm; solvent = 1:10 pyridine:toluene; concentration = 5 × 10^{-6} M.

absorption at longer wavelength. Clear isosbestic points are seen in the spectra, indicating that only one photoexcited species was formed. T_n-T_1 energy gaps are reported in Table 2.

Phosphorescence spectra were obtained for these compounds; the excitation wavelength in each case corresponded to the red edge of their respective 0−0 absorption bands. The values for phosphorescent emission maxima along with the first excited singlet-to-lowest excited triplet energy gaps are given in Table 2.

Discussion

The development of a comprehensive picture regarding how efficient, directional excitation transfer is effected in the biological antenna systems, as well the potential evolution of true molecular electronic devices and a new generation of photonic materials, has driven a great deal of the current research in multichromophoric assemblies. To achieve these ambitious objectives, fundamental insights into the nature of the coupling of chromophores to the bath (protein, solvent) as well as to how this differs from interchromophore communication must be obtained. In this light, our research goals in this area focus on (i) understanding how energy is disposed of once it is captured in a multichromophoric system and (ii) characterizing the nature of electronic communication between chromophores in multiporphyrin arrays as a function of interchromophore distance, orientation, and ground-state electronic coupling, as well as upon the magnitudes of the transition dipole moments and excited-state anisotropy of the supermolecule.

Zero Field Splitting Parameters, Symmetry Considerations, and the Extent of Delocalization. EPR spectroscopy of lowest energy metastable triplet state can provide information regarding the magnitudes of both electronic communication and delocalization between the chromophores that compose these multichromophoric arrays as well as the time scales that govern these interactions.[53] The ZFS parameters, D and E, can be related to the overall distribution of the two-center spin contributions of the metastable triplet state. The $|D|$ ZFS permits an estimate of the extent as well as the geometrical shape of the spin distribution through the following expressions:

$$D = \frac{3}{4}\left(\frac{\mu_o}{4\pi}\right)(g_e\beta_e)^2\left\langle\frac{r^2 - 3z^2}{r^5}\right\rangle \text{ or}$$

$$= \frac{3}{4}\left(\frac{\mu_o}{4\pi}\right)\frac{(g_e\beta_e)^2}{r^3}\langle 1 - 3\cos^2\theta\rangle \quad (3)$$

Here, r is the magnitude of the distance between spin centers, x, y, and z are the distances between spin centers projected onto the principal axis system of the molecule, and θ is the polar angle describing the relative orientation of the dipoles. The essential features can be qualitatively seen by looking at the $\langle r^2 - 3z^2\rangle$ term of D. The expression $\langle r^2 - 3z^2\rangle$ or $\langle x^2 + y^2 - 2z^2\rangle$ is positive ($D > 0$) for an oblate distribution of spin, as one would expect for a flat planar aromatic molecule, and $\langle x^2 y^2 - 2z^2\rangle$ is negative ($D < 0$) for a prolate spin distribution, as is often observed for linear molecules. Relating this to the expression in polar angle θ, the extremum at $\theta = (\pi/2)$, ($D > 0$), corresponds to a side-by-side triplet spin alignment, while that at $\theta = 0$, ($D < 0$), corresponds to a head-to-tail spin alignment. Thus, at a fixed center-to-center distance, r, the limiting cases give $|D(\theta = 0)| = 2|D(\theta = \pi/2)|$. For planar aromatic molecules, $\langle z\rangle \ll \langle r\rangle$, and hence, the expression for D reduces to

$$D \cong \frac{3}{4}\left(\frac{\mu_o}{4\pi}\right)(g_e\beta_e)^2\frac{1}{\langle r^3\rangle} \quad (4)$$

Therefore, D can be used as a gauge of the average interelectron distance between electrons occupying the triplet molecular orbital.

The E ZFS parameter given in the following expression

$$E = \frac{3}{4}\left(\frac{\mu_o}{4\pi}\right)(g_e\beta_e)^2\left\langle\frac{(y^2 - x^2)}{r^5}\right\rangle \quad (5)$$

permits an assessment of the in-plane spin anisotropy. Typically, for molecules possessing 3-fold or higher rotational symmetry, $\langle y^2 - x^2\rangle$ vanishes, giving an E value of zero and an axially symmetric EPR line shape (excluding Jahn−Teller effects). Despite the fact that the E ZFS parameter provides crucial information regarding the nature of the triplet excited state, this variable has rarely been determined and/or discussed for supermolecules composed of more than a single porphyrin unit.

Monomers. The line shape of the EPR spectra of the photoactivated triplet state of ZnDPP (**1**), ZnTPP (**5**), and their monomeric ethyne- and butadiyne-elaborated derivatives (**2**−**4**, **6**, **7**) all exhibit rhombic symmetry ($|D| \geq 3|E|$). For ZnDPP (**1**) and ZnTPP (**5**), $|D| \sim 3|E|$ is due to JT effects, and consequently, the high- and low-field Z transitions contain overlapping resonance contributions from the two canonical orientations (Z and Y). In ZnTPP, the excited triplet state is spatially doubly degenerate and has a representation of ^3E_u in the D_{4h} point group. It is thus susceptible to Jahn−Teller instability; given perturbations that have their genesis in crystal-field interactions, the degeneracy is relieved, yielding two triplet states separated by an energy gap (δ_{JT}). When $k_BT < \delta_{JT}$ a

(53) (a) Levanon, H.; Norris, J. R. *Chem. Rev.* **1978**, *78*, 185−198. (b) Gonen, O.; Levanon, H. *J. Chem. Phys.* **1986**, *84*, 4132−4141. (c) Thurnauer, M. C.; Norris, J. R. *Chem. Phys. Lett.* **1980**, *76*, 557−561. (d) Closs, G. L.; Forbes, M. D. E.; Norris, J. R. *J. Phys. Chem.* **1987**, *91*, 3592−3599. (e) Norris, J. R.; Morris, A. L.; Thurnauer, M. C.; Tang, J. *J. Chem. Phys.* **1990**, *92*, 4239−4249. (f) Wasielewski, M. R.; Gaines, G. L., III; O'Neil, M. P.; Niemczyk, M. P.; Svec, W. A. *J. Am. Chem. Soc.* **1990**, *112*, 4559−4560.

Table 2. Comparative Phosphorescence Emission and $T_1 \rightarrow T_n$ Absorption Data for the Monomeric, Dimeric, and Trimeric (Porphinato)zinc Complexes

	compd	wavelength ($\lambda_{max\ 1,nm}$)	wavelength ($\lambda_{max\ 2,nm}$)	$\Delta E(S_1 - T_1)^a$ (cm^{-1})	$\Delta E(T_n - T_1)^b$ (cm^{-1})
1	ZnDPP	758	851	2531 5285	
5	ZnTPP	791	889	3942 4077	21 322[72a]
2	5-ethynyl-ZnDPP	815	839	4062 3269	21 448
3	5,15-diethynyl-ZnDPP	888	915	4361 3564	20 632
7	2,12-diethynyl-ZnTPP	831	938	4121	20 538
8	*meso*-to-*meso* ethyne-bridged dimer	*c*	*c*	*d*	19 528
9	*meso*-to-*meso* butadiyne-bridged dimer	*c*	*c*	*d*	19 486
10	*meso*-to-*meso* ethyne-bridged trimer	*c*	*c*	*d*	18 808
11	β-to-β ethyne-bridged dimer	817	911	3633 3600	19 110
12	β-to-β butadiyne-bridged dimer	827	929	4009 4134	19 422
13	β-to-β butadiyne-bridged trimer	855	*c*	4077	18 787
14	*meso*-to-β ethyne-bridged dimer	825	933	3146	20 328
15	*meso*-to-β butadiyne-bridged dimer	861	913	3830	19 233

[a] The first entry in this column for a given compound corresponds to the S(0,1) − T(0,1) gap, while the second entry represents the S(0,0) − T(0,0) energy separation. Note that for compounds exhibiting phosphorescence, the $T(0,0)$ emission is not always observed. [b] $T_1 \rightarrow T_n$ excitation energies were obtained from absorption spectra recorded 100 ns after the pump pulse. [c] No well-resolved peaks detected. [d] No phosphorescence observed.

nonaxial symmetric spectrum results; as k_BT becomes comparable or exceeds δ_{JT}, the line shape becomes temperature dependent with the emergence of an axially symmetric EPR spectrum. Such is the case for ZnTPP, where at low temperature the EPR spectrum displays almost complete rhombic symmetry ($|D| \sim |3|E$, Table 1). EPR spectra obtained at higher temperatures for ZnTPP have shown that by 100 K there is a significant contribution from the axially symmetric component. At this temperature, the spectrum does not show complete coalescence, and consequently, the maximum δ_{JT} can be estimated to be >150 cm^{-1}. For ZnTPP, both EPR and resonance Raman spectroscopic studies concur that there are no significant conjugative interactions between the *meso*-aryl groups and the porphyrin macrocycle.[54]

ZnDPP displays a low-temperature EPR spectrum that can be also interpreted using the D_{4h} point group as the reference point for departure. The finding that ZnDPP shows the same symmetry in its EPR spectrum as ZnTPP is consistent with the view that porphyrin *meso*-phenyl substituents do not appreciably extend the porphyrin π-system, and thus do not perturb the ZFS parameters of the porphine metastable triplet state. Analysis of the temperature dependence of the EPR spectral line shape shows that the onset of the axial component for ZnTPP occurs at higher temperature than observed for ZnDPP, indicating that δ_{JT} is larger for the tetra-*meso*-substituted porphyrin. As can be seen from Figure 3A, the emergence of an axial triplet component ($E \approx 0$) is clearly evident at 20 K and contributes a significant proportion of the total intensity in the X−Y region by 100 K, signifying that for ZnDPP δ_{JT} is ≤ 100 cm^{-1} for a large proportion of the ZnDPP molecules in the glassy matrix. This gradual onset of the axial component results directly from the fact that within a glassy matrix there exists a distribution of δ_{JT} energy splittings, and thus, the EPR spectrum is a composite of molecules that possess varying amounts of axial and nonaxial spectral signatures over a broad temperature range.[45,47,52] Thus, ZnDPP, like ZnTPP, possesses a triplet excitation adequately described within the D_{4h} point group (C_{4v} if ligation is considered; this, however, does not affect the degeneracy of the triplet excited state) and also exhibits a temperature dependent EPR line shape described by dynamic JT phenomena.

(54) de Paula, J. C.; Walters, V. A.; Nutaitis, C.; Lind, J.; Hall, K. *J. Phys. Chem.* **1992**, *96*, 10591−10594.

As seen from the magnitudes of the $|D|$ ZFS parameters listed in Table 1, direct attachment of ethynyl and butadiynyl groups to the porphyrin *meso* or β positions does not grossly perturb the spatial relationship of the electrons in the triplet excited state relative to both ZnTPP and ZnDPP. Moreover, for molecules **2**−**4**, **6**, and **7**, the EPR line shape yields ZFS parameters essentially invariant with respect to temperature (e.g., Figure 3B), with no evidence of the emergence of an axial triplet up to temperatures approaching the glass transition temperature ($T \approx 120$ K). The $|E|$ ZFS parameter, on the other hand, demonstrates that increasing conjugation at the porphyrin periphery in compounds **2**−**4**, which bear 5-ethynyl, 5- and 15-ethynyl, as well as 5- and 15-butadiynyl groups fused to the ZnDPP skeleton, respectively, results in increasing $|E|$ values that approach an extreme asymmetry value of $3|E|/|D| = 1$. This trend shows that increasing the extent of conjugation at the *meso*-carbon position results in enhanced in-plane anisotropy of the spin-density. Optical spectroscopy of **2**, **3**, and **7** corroborates a reduction in excited state symmetry;[31] for example, compound **3**, which bears two ethynyl groups fused to the porphyrin 5- and 15-positions, has an electronic spectrum consistent with the removal of the degeneracy of the *x*- and *y*-polarized excited states and shows a 500 cm^{-1} splitting between the B_x and B_y transitions. Likewise, the EPR spectrum of the photoactivated triplet state of **3** clearly shows a triplet spectrum with rhombic symmetry ($3|E|/|D| = 0.5$); furthermore, the temperature dependence of the EPR signal demonstrates that the effective symmetry of the lowest excited triplet is less than D_{4h}. The optical and photophysical properties of **2**, which bears a single ethyne group at the porphyrin 5-position, and **7**, which possesses two ethynyl groups fused to the macrocycle 2- and 12-positions, evince energetic differences between the B_x and B_y states, though the splitting of the *x*- and *y*-polarized transitions is considerably less than that observed for **3**.[31,33] Consistent with the experimentally observed reduction in symmetry for the photoexcited singlet states of molecules **2** and **7**, the photoactivated EPR triplet spectra for these species display line shapes typical of rhombic symmetry, with $3|E|/|D|$ equal to 0.457 and 0.911, respectively. Figure 3B illustrates the temperature dependence of the photoactivated triplet EPR spectrum of 2,-12-diethynyl-ZnTPP (**7**) (Figure 2B), exemplifying the significant deviation from an axially symmetric spectrum for these

compounds that is observed over a large temperature range. The temperature dependence of the EPR spectra of **2**, **3**, **6**, and **7** (Figure 3B), moreover, all demonstrate no tendency to evolve into a line shape with an $E \sim 0$ component indicating that covalent attachment of a single ethynyl group at the porphyrin *meso* or β position effects sufficient symmetry breaking to relieve the JT instability completely or serves to increase the magnitude of δ_{JT} such that a temperature beyond the glass transition of the solvent is required to effect the coalescence of the X and Y canonical transitions. Due to the similarity in the EPR line shape and ZFS parameters of the β-ethyne-elaborated ZnTPP derivatives (**6** and **7**), with that of the parent molecule, ZnTPP, we cannot eliminate the possibility that the symmetry of the triplet molecular orbital may contain a C_4 element and that the δ_{JT} is $\gg 150$ cm^{-1} ($2k_BT$ at 100 K), well beyond the temperature accessible in this glass matrix. It is clear, over the temperature range probed, that the triplet excitation in all the ethyne-elaborated monomers (**2**, **3**, **6**, **7**) maintains rhombic symmetry with no evidence of the dynamic JT effect.

Dimers and Trimers. For the dimeric and trimeric (porphinato)zinc(II) arrays (excluding compound **9**), the data presented in Table 1 show that the ZFS parameter $|D|$ is only slightly smaller in magnitude than that observed for the monomeric porphyrin molecules (**1**−**7**). Even the most highly conjugated array in the series, **10**, which has by far the lowest $\pi \rightarrow \pi^*$ gap,[31−33] has a $|D|$ value only 7% smaller than that measured for its parent porphyrin structure ZnDPP. Furthermore, the $|D|$ value for the *meso*-to-*meso* ethynyl-bridged trimer **10** is only four percent smaller than that observed for the *meso*-ethynyl derivative of ZnDPP (**3**). The EPR data are thus consistent with a picture that describes the triplet excitation as *localized* on a single (porphinato)zinc unit within these multiporphyrin arrays and not generally delocalized over the entire molecule; this is the case regardless of the bridge topological structure and the mode of chromophore-chromophore connectivity.[55]

The EPR spectrum of the *meso*-to-*meso* ethyne-bridged dimer **8** changes little as a function of temperature (Figure 5A) with respect to both the ZFS parameters and overall line shape. The EPR spectral data for **8** is similar to that obtained for porphyrin arrays **9**−**15**, which all show no evidence of dynamic JT interactions up to the glass transition temperature; consequently, all EPR spectra demonstrated rhombic symmetry with $|D| \geq 3|E|$ in most cases with no evidence of axial triplet components ($E \sim 0$).

All of the ethyne- and butadiyne-bridged porphyrin arrays exhibit phenomenally large excitonic coupling in the S_2 state,[31−33] consistent with (i) close interspatial separation of the chromophores, (ii) large coupling enabled by the ethyne and butadiyne moieties that wire the macrocycles together, and (iii) the fact the constituent porphyrinic components of the arrays have enormous associated electronic transition moments. For the porphyrin-to-porphyrin ethyne-bridged supermolecules, the magnitude of conjugative interactions that are enabled are greatest for the *meso*-to-*meso* linkage topology, followed by β-to-β and *meso*-to-β connectivities; for the butadiyne-bridged chromophore systems, the order is *meso*-to-*meso* > *meso*-to-β > β-to-β.[32] None of the arrays have optical features that can be interpreted as the simple superposition of the electronic spectra of the constituent porphyrinic building blocks of the supermolecule. It might have thus been expected based on the photophysical properties of the singlet states of these molecules that the $|D|$ value would be highly variable throughout this series of conjugated porphyrins, with its magnitude inversely correlated with the extent of electronic delocalization in the supermolecule evaluated by both electrochemical and optical methods.[31−33] That such an effect is not observed delineates distinct differences exist between the physical properties of the singlet- and triplet-excited states of these highly conjugated porphyrin arrays.

Optically detected magnetic resonance and triplet EPR studies on noncovalently linked cofacial chlorophyll dimers and covalently linked face-to-face pyrochlorophyll dimers demonstrate ZFS parameters and triplet state kinetics similar to that of their parent chromophores.[56] These results are not inconsistent with Kasha's point dipole exciton model. Within this theoretical framework, it has been determined that when the electronic coupling for a dimeric species is larger than the ZFS, the spin Hamiltonian describing the triplet state is the average of the spin Hamiltonians of the constituent monomers. In the strong coupling limit, intermolecular interactions force quantization of the spin axes along the dimer principal axes that are the average with respect to the principal axes of the two monomeric constituents; such a model has been verified in molecular crystal systems.[57] For cofacial dimeric chromophores systems triplet exciton theory will always predict that $D_{dimer} \leq D_{monomer}$; thus, the theory cannot account for an increase in the D value of bis(chromophore) complexes relative to their parent precursor molecules.

Amid the predictive power of the triplet exciton model there are situations when its application is inappropriate. First, the interpretation of EPR triplet spectra with exciton theory is predicated on the exchange interaction (charge resonance in a homodimer or charge transfer in a heterodimer) being small compared to the zero field splitting ($J < D$). As increased exchange interaction occurs ($J > D$), one must take into account charge transfer interactions, which have been demonstrated to cause a reduction in the $|D|$ ZFS parameter and an increase in triplet decay kinetics. In such a case, the exciton theory predicted relationship of the ZFS parameters to the triplet excited-state electronic spatial distribution is no longer valid. Second, experiments indicate that this model does not hold for many systems where one would think that interpretation of the triplet spectrum would be straightforward. For instance, van Willigen[58] and Gückel[59] have demonstrated that triplet kinetics and EPR spectra of cofacial porphyrin dimers were essentially invariant with respect to the monomeric precursors, making it difficult to rationalize these data in terms of face-to-face bis(porphyrin) structures possessing *perfectly* coincident principal axis systems. van Willigen has proposed that in these cases triplet excitation is indeed localized on a single chromophore of the bis(chromophore) system.[60] Furthermore, in the bacterial reaction center in *Rhodopseudomonas virdis*, Norris has determined that the triplet excitation is almost completely localized on the L-subunit portion of the special pair dimer.[61] Likewise, Möbius and co-workers have recently employed time-resolved

(55) These results also imply that the extent of electronic delocalization within the triplet excited state for these highly-conjugated porphyrin arrays is not strongly correlated with chromophore-chromophore torsional barriers to rotation. See ref 32.

(56) Clarke, R. H.; Hobart, D. R.; Leenstra, W. R. *J. Am. Chem. Soc.* **1979**, *101*, 2416−2473.

(57) (a) Sternlicht, H.; McConnell, H. M. *J. Chem. Phys.* **1961**, *35*, 1793−1800. (b) Jortner, J.; Rice, S. A.; Katz, J. L.; Choi, S.-I. *J. Chem. Phys.* **1965**, *42*, 309−323. (c) Hochstrasser, R. M.; Lin, T.-S. *J. Chem. Phys.* **1968**, *49*, 4929−4945. (d) Haarer, D.; Wolf, H. C. *Mol. Cryst.* **1970**, *10*, 359−380.

(58) Chandrashekar, T. K.; van Willigen, H.; Ebersole, M. H. *J. Phys. Chem.* **1984**, *88*, 4326−4332.

(59) Gückel, F.; Schweitzer, D.; Collman, J. P.; Bencosme, S.; Evitt, E.; Sessler, J. *Chem. Phys.* **1984**, *86*, 161−172.

(60) Chandrashekar, T. K.; van Willigen, H.; Ebersole, M. H. *J. Phys. Chem.* **1985**, *89*, 3453−3459.

(61) Norris, J. R.; Budil, D. E.; Gast, P.; Chang, C.-H.; El-Kabbani, O.; Schiffer, M. *Proc. Natl. Acad. Sci. U.S.A.* **1989**, *86*, 4335−4339.

EPR spectroscopy to investigate triplet energy transfer in a series *o*- and *p*-phenylene-linked porphyrin dimers;[62] in all the dimers studied, the ZFS parameters were similar to the monomeric ZFS values, forcing these workers to the conclusion that on the time scale sampled by EPR, the triplet excitation was localized on one half of the dimer and consequently the electronic interaction between the porphyrins is weak.[62] When spin-lattice relaxation measurements were obtained these systems, excitation transfer rates on the order of 5×10^9 s^{-1} were observed, suggesting that this process occurred in the intermediate to slow exchange limit.

Of the compounds studied in this work, only the arrays with a *meso*-to-*meso* ethynyl and butadiynyl linkage topology, **8**–**10**, have photophysical and optical properties consistent with near-maximized interchromophore conjugation in solution.[31-33] Consequently, such structures would have a rigorous C_2 axis of symmetry with at least one of their principal axes coincident with the supramolecular C_2 symmetry axis.[61] Of the ethyne-bridged porphyrin arrays (**8**, **10**, **11**, **14**), only **8** and **10** exhibit an EPR line shape for the photoexcited triplet that differs significantly from that seen for the monomeric porphyrins **1**–**7** (Figures 1, 2, and 4). Optical spectroscopy has revealed extremely large excitonic splittings in the B-band regions of compounds **8** and **10** as well as substantially red-shifted Q-band absorptions relative to ZnDPP;[31] furthermore, fluorescence anisotropy measurements of **8** and **10** recorded at 20 ps after excitation show that the fluorescent excited state is nondegenerate and polarized along the C_2 molecular axes of highest conjugation.[33] These studies show that **8** and **10** exhibit enormous interchromophore electronic coupling in their respective singlet-excited states; moreover a point-dipole analysis of their optical spectra corroborates a description of these systems in which the porphyrin–porphyrin geometrical relationships within the supermolecule are approximately coplanar.

As previously demonstrated, the magnitude of the E value correlated with the extent of conjugation in compounds **2**–**4**. In **4**, which bears two *meso*-butadiynyl groups, an asymmetry value of 0.816 was obtained; this contrasts the asymmetry values of 0.457 and 0.528 obtained for the 5-ethynyl and 5,15-diethynyl derivatives of ZnDPP (**2** and **3**), respectively. Extrapolating this trend, we argue that increasing the in-plane asymmetry through augmented chromophore–chromophore conjugation in these arrays will eventually generate a molecule where the direction of largest dipolar interaction (taken as the *Z*-direction, arbitrarily), is no longer perpendicular to the molecular plane but along the C_2 axis of highest conjugation in the multiporphyrinic array. In the *meso*-to-*meso* ethyne-bridged dimer (**8**) and the *meso*-to-*meso* butadiyne-linked dimer (**9**) we see compelling evidence of this transition occurring. That is, in **8** we postulate that the direction of the largest dipolar interaction is now along the vector defined by the *meso*-to-*meso* carbon connectivity and that the spin distribution has become prolate in nature as opposed to the oblate distribution observed in the monomeric porphyrins. Given this transition of oblate-to-prolate spin distribution, the $|D|$ value for a fixed interelectron distance would be predicted by theory to increase by a factor of 2 (eq 4). For **8**, the magnitude of the $|D|$ value indicates that if the triplet spin density is localized predominantly on one of the ZnDPP units of the dimer, the interelectron distance must have increased relative to molecules **1**–**4**. This augmentation of the interelectron distance with the oblate-to-prolate spin transition accounts for the $|D|$ ZFS parameter of **8** increasing only slightly compared to ethyne-and butadiyne-elaborated (porphinato)zinc monomeric species **2**–**4**. This type of spin orientation also accounts for the more substantial increase in $|D|$ observed for the *meso*-to-*meso* butadiyne bridged dimer **9** relative to monomeric porphyrins **1**–**7**. For compound **9**, the $|D|$ value is 0.0447 cm^{-1} as compared to 0.0326 cm^{-1} for the parent (porphinato)zinc complex ZnDPP. Using eq 5, we can estimate that the interelectron distance increases from 3.5 to 4.0 Å on going from ZnDPP to the *meso*-to-*meso* butadiyne-bridged array. Moreover, the expansion of the interelectron distance within the photoactivated triplet state from 4.0 Å in **9** to 4.3 Å in **8** shows that this property correlates quite closely with the extent of both excitonic and electronic coupling between the ZnDPP building blocks of these arrays evinced in their optical spectra.[31,32] Although these represent only modest changes in interelectron distance in **8** and **9** with respect to ZnDPP, the trend that greater photoactivated triplet state electronic delocalization correlates with enhanced chromophore–chromophore coupling for these highly conjugated, symmetric dimeric porphyrin systems is noteworthy; we hypothesize that this effect will be magnified in structurally analogous, higher order (porphinato)zinc arrays that have been engineered to exhibit such prolate spin distributions.

Similar data indicating an oblate-to-prolate triplet spin redistribution were encountered for the 22π and 26π acetylene–cumulene (stretched) porphycenes; these species possess magnified $|D|$ values relative to the parent porphycene structure, and consequently an in plane spin realignment along the highly conjugated axis was postulated.[63] Further EPR studies of **8**- or **9**-based systems involving (i) the engineering of inequivalent environments about the ZnDPP constituent chromophores (through chemical means or by introduction of the chromophore in an appropriate liquid crystal environment), (ii) photoactivated triplet EPR magnetophotoselection studies, or (iii) the synthesis and spectroscopy or higher order arrays featuring a *meso*-to-*meso* ethynyl or butadiynyl linkage topology will serve to further characterize how conjugation length, conjugation mode, and chromophore geometry impact both interelectron separation and the oblate-to-prolate spin redistribution event originally hypothesized by Levanon.[63]

Although not proven, it seems unlikely that triplet spin migration in the *meso*-to-*meso* ethyne-bridged arrays occurs on the time scale probed in this study, since breaking symmetry in the bis[(porphinato)zinc] chromophore **8** requires only asymmetric solvation about the ZnDPP units of the dimer. For example, optical spectroscopy shows that even small changes in the solvation environment produce large inhomogeneous broadening for organic molecules in solution.[64,65] Although disparate solvation environments about the ZnDPP units of the highly conjugated trimeric porphyrin array **10** may play a role in symmetry breaking, the central ZnDPP monomer is electronically unique and likely provides the primary driving force for triplet localization within the array. EPR studies of one-electron oxidized assemblies of weakly coupled (porphinato)zinc and free-base porphyrin molecules linked by diarylethyne units show a lack of hyperfine resolution in their higher order arrays.[66] This was interpreted in terms of spin migration occurring on the order of 10^7 s^{-1} or faster in solution, with a significantly slower rate in the frozen state determined by rate-limiting solvation effects.

(62) Jaegermann, P.; Plato, M.; von Maltzan, B.; Möbius, K. *Mol. Physics* **1993**, *78*, 1057–1074.

(63) Berman, A.; Levanon, H.; Vogel, E.; Jux, N. *Chem. Phys. Lett.* **1993**, *211*, 549–554.

(64) Personov, R. I. In *Site Selection Spectroscopy of Complex Molecules in Solutions and Its Applications*; Agranovich, V. M., Hochstrasser, R. M., Eds.; North-Holland Publishing Co.: Amsterdam, 1983; pp 555–619.

(65) Logovinsky, V.; Kaposi, A. D.; Vanderkooi, J. M. *Photochem. Photobiol.* **1992**, *57*, 235–241.

(66) Seth, J.; Johnson, T. E.; Prathapan, S.; Lindsey, J. S.; Bocian, D. F. *J. Am. Chem. Soc.* **1994**, *116*, 10578–10592.

Moreover, for electronically asymmetric arrays, exemplified by a porphyrin−(porphinato)zinc bis(chromophore) system featuring a diarylethyne bridging moiety, the cation-radical EPR spectra is consistent with hole localization on the (porphinato)zinc unit.

Electrochemical experiments, optical spectroscopy, and photophysical studies show that the β-to-β ethyne- and butadiyne-bridged dimeric and trimeric porphyrin arrays (**11**−**13**) are much less strongly conjugated than analogous arrays with *meso*-to-*meso* connectivity. This derives in part from the increased steric interactions between the constituent chromophores of the array that are due to tetrakis(*meso*-aryl) substitution as well as the fact that β-to-β carbon connectivity effects less efficient (porphinato)zinc−(porphinato)zinc electronic coupling with respect to a *meso*-to-*meso* bridging motif that involve either ethyne or butadiyne moieties.[31−33] The photoexcited triplet EPR spectra recorded at 4 K for **11**, **12**, and **13** (Figure 7) demonstrate quite clearly that the line shape obtained varies little with respect to both ZnTPP and its 2-ethynyl and 2,12-diethynyl elaborated derivatives **6** and **7**. The $|D|$ ZFS parameters of these arrays, likewise, are all within 4% of that seen for molecules **6** and **7**.

The low temperature EPR spectra of the *meso*-to-β dimeric arrays **14** and **15** are intriguing. Compound **14**, in which an ethynyl moiety bridges ZnDPP and ZnTPP chromophores at their respective *meso* and β carbon atoms, shows a 4 K EPR spectrum that demonstrates the existence of two triplets possessing $|D|$ values of 0.0283 and 0.0313 cm^{-1}. Compound **15**, the butadiyne-bridged dimeric analogue of **14**, demonstrates a single triplet species whose $|D|$ ZFS parameter is 0.0351 cm^{-1}, larger than all the porphyrin monomers and arrays studied, excepting the *meso*-to-*meso* butadiyne bridged dimer **9**. Again, a likely explanation for the magnitude of the D value of compound **15** is that spin realignment has taken place; the observed $|D|$ ZFS parameter, however, is only slightly greater than that seen for ZnTPP making it difficult to conclude that an oblate-to-prolate spin transition has indeed taken place.

Temperature Dependent Profiles of Electron Spin Polarization and Relaxation. Electron spin polarization is demonstrated by all the compounds in this study and provides considerable insight into the mechanism of intersystem crossing from the first excited singlet state. Double modulation studies made popular by Levanon[67] and van Willigen[68] have exploited the enhanced signal to noise provided by non-Boltzmann filling of the triplet manifold to study the kinetics of population and depopulation of the triplet sublevels at temperatures typically in excess of 100 K, where steady state light illumination renders an EPR spectrum of a thermalized triplet manifold. For porphyrinic species studied at 4 K, the relative magnitudes of the triplet lifetimes and electron spin lattice relaxation time (T_1) are such that even with steady state illumination, Boltzmann equilibration among the triplet spin sublevels is not established. This accounts for the observation of both the enhanced absorptive and emissive signals in the photoactivated triplet EPR spectra. Following methods described by Thurnauer,[42] the relative intensity pattern can be predicted from the initial population or depopulation rates; similarly, the relative population and depopulation rates may be inferred from the spin polarization pattern. The observation of spin polarization with a polarization pattern of **aaa eee** or **a-a e-e** has been noted for compounds **1**−**7** and **10**−**15**. This polarization pattern is consistent with ISC occurring predominantly by way of the $|T_z\rangle$ spin sublevel following the convention that the triplet spin sublevels have the ordering: $|T_x\rangle > |T_y\rangle > |T_z\rangle$. Furthermore, this result is in accord with those obtained for other (porphinato)zinc complexes[45] and is consistent with the triplet mechanism enabled by spin−orbit coupling.

In compounds **8** and **9**, where we have proposed that spin realignment occurs along the molecular C_2 axis of highest conjugation and that the polarization pattern is aae aee, the D would be negative and the relative energy ordering of spin sublevels would be $|T_z\rangle > |T_x\rangle, |T_y\rangle$.[53a]

The persistence of electron spin polarization under steady state illumination is seen in **3** (data not shown) and **7** well above 90 K (Figure 3B). Compounds **1** (Figure 3A) and **5** (data not shown), however, are undergoing thermalization at 70 K while **3** shows only a minor departure from a nonthermal Boltzmann distribution at 70 K (data not shown). Although this effect may be due to the fact that the phosphorescent lifetimes of the ethynyl-derivatized porphyrins are less than that observed for either ZnDPP and ZnTPP, it is difficult, however, on data based on lifetime arguments alone, to reconcile the persistence of electron spin polarization over such a large temperature excursion without postulating a weak temperature dependence of the spin-lattice relaxation time.

As shown in Figure 5A, **8** reveals little change in line shape as a function of temperature. One of the most unusual features of this temperature dependence is the fact that little thermalization is evident over a 4−70 K range under conditions of steady state illumination. It is evident for **9** (Figure 5B) that thermalization is not observed for either the major or minor triplet species ($|E|$ values = 0.0097 and 0.0092 cm^{-1}, respectively). Since both species possess the same $|D|$ value, thus having identical electronic spatial distributions, the two triplet species differ only slightly in their extent of distortion from tetragonal symmetry, suggesting that these two triplet species may correspond to closely related geometrical isomers.

The nature of the temperature dependence of triplet state spin-lattice relaxation in glassy matrices does not conform to models predicted by theory for various relaxation processes and has been debated over the past several years.[69] Recently, Gradl[70] has put forth an extension of the original theory of Bowman and Kevan[71] to explain the weak temperature dependence of the triplet spin lattice relaxation times in amorphous and glassy systems. In these theories, the coupling of the spin system to the disorder (two-level system) modes is thought to be stronger than the more traditional spin−phonon coupling resulting in temperature dependencies that exhibit temperature−power laws on the order of 1−2. As can be seen from Figure 6 and its inset, the temperature dependence of the saturation parameter, $P_{1/2}$, obtained from the analysis of progressive power saturation measurements (a measure of temperature dependence of $1/T_1$) clearly demonstrates the weak temperature dependence of spin lattice relaxation.[49,50] Since the power saturation characteristics of **8** were studied at only four temperatures over a 4−50 K temperature range, it is impossible to evaluate exactly the temperature exponent; however, it clearly lies in the range $1 \leq n \leq 2$ and therefore is consistent with the theory put forth by Gradl and Friedrich, in which the triplet spin is more strongly coupled to the disorder modes rather than the phonon modes.[70] Analysis of the data using this model also gave a b factor of 1.70 ± 0.02 for all four temperatures, indicating that the line shape is not purely homogeneously broadened ($b = 3$), nor is it in the inhomogeneously broadened limit ($b = 1$) as is commonly observed for chromophores in a glassy matrix.[49,50]

(67) Levanon, H.; Weissman, S. I. *Isr. J. Chem.* **1972**, *10*, 1−5.
(68) Pandian, R. P.; Chandrashekar, T. K.; van Willigen, H. *Chem. Phys. Lett.* **1992**, *198*, 163−167.
(69) Kaiser, G.; Pierron, H.; Friedrich, J. *J. Chem. Phys.* **1993**, *99*, 605−609.
(70) Gradl, G.; Friedrich, J.; Kohler, B. E. *J. Chem. Phys.* **1986**, *84*, 2079−2083.
(71) Bowman, M. K.; Kevan, L. *J. Phys. Chem.* **1977**, *81*, 456−461.

The EPR temperature profile of the photoactivated triplet state of the *meso*-to-β ethyne-bridged bis[(porphinato)zinc] complex **14** (Figure 9) also shows little thermalization under steady state illumination up to and above 50 K. Interestingly, the line shape demonstrates the loss of signal due to triplets with a $|D|$ value of 0.0313 cm^{-1}. The low-temperature line shape is thus a composite of two triplet species; the line shape changes that occur with increasing temperature have been observed to be reversible, potentially consistent with a dynamic interconversion between two different conformers of **14** that each exhibit a unique photoactivated triplet EPR spectrum. Similar line shape changes with temperature have been observed for the photoactivated triplet EPR spectra of **9**, where increasing temperature results in a decrease in relative intensity for the triplets with an $|E|$ value of 0.0092 cm^{-1} (Figure 5B).

In contrast, the *meso*-to-β butadiyne-bridged dimer **15** exhibits temperature-dependent triplet EPR spectra consistent with immobile triplet excitation. Such an effect could derive in part from the slightly longer interchromophore distance in **15** relative to **14**. Since similar effects were not observed for the *meso*-to-*meso* ethyne- and butadiyne-bridged (porphinato)zinc complexes **8** and **9**, nor were they observed for the analogous β-to-β coupled derivatives **11** and **12**, (porphinato)zinc−(porphinato)zinc distance is not a probable cause of immobile triplet excitation. It is more likely that **14**'s temperature dependent EPR spectrum derives from its unique interchromophore geometry. Previous work has shown that the *meso*-to-β ethyne-bridged (porphinato)zinc dimer is essentially locked in a geometry in which the porphyrin−porphyrin torsional angle is 90°; substantial steric interactions permit only relatively small librations about this conformational minimum.[32] The mutually orthogonal relationship of the chromophores enables minimal communication between the porphyrin π systems and is thus consistent with the observation of two $|D|$ values of 0.0283 and 0.0313 cm^{-1} for the *meso*-to-β ethyne-bridged dimer; these parameters correspond to what would be observed in the photoactivated triplet EPR spectrum of a sample containing a mixture of the β-ethynyl-derivatized ZnTPP (**5**) complex with the *meso*-ethynyl-derivatized ZnDPP (**3**) species. Molecule **14** is a unique member of this series of highly conjugated (porphinato)zinc arrays since its constituent ZnDPP and ZnTPP building blocks are completely decoupled at low temperature. Presumably, as the temperature is increased from 4 K, enhanced librational motion about the ethyne bond enables small but finite coupling between the ZnDPP and ZnTPP units of the dimer; this results in the triplet emission becoming localized on the (porphinato)zinc unit (2-ethynyl-ZnTPP) with the lowest triplet energy (Table 2).

Optical Properties of the Photoactivated Triplet State. The transient triplet-triplet ($T_1 \rightarrow T_n$) electronic spectra (Figure 10) for the *meso*-to-*meso* ethyne-bridged arrays evince significant absorptive components to the blue of their Q-type transitions as well as at high energy (~350 nm). The wavelength regime corresponding to the B-band bleach in these complexes clearly indicates that the T_1 state absorbs little, if at all, in this spectral region. The strong absorbances at 512 and 531.7 nm observed for compounds **8** and **10**, respectively, are of similar shape and intensity to the analogous $T_1 \rightarrow T_n$ absorption observed for ZnTPP and suggest that this transition corresponds to a doubly excited electronic configuration. This hypothesis is in accord with the known $^3(\pi,\pi^*)$ spectra of simple (porphinato)zinc complexes which are consistent with a T_n state having an electronic configuration of $a_{1u}^1a_{2u}^1e_g^1e_g^1$ (a doubly-excited four orbital electronic state) rather than a higher singly excited configuration (e.g., $a_{1u}^1a_{2u}^2e_g^0e_g^0b_{1u}^1$).[72] The $T_1 \rightarrow T_n$ excitation thus involves the promotion of a second electron from an orbital that is filled in the ground-state; this transition occurs in the blue region of the spectrum signifying that the electronic system of the T_1 state is not severely distorted with respect to the S_0 state of ZnTPP.[72b] Whether or not the photoactivated triplet states of **8**, **10**, and the remainder of these conjugated porphyrin arrays can be described in the context of a classic Gouterman four-orbital picture is an open question, particularly given that the electronic spectra and photophysical properties of many of these species are consistent with a significant splitting of the *x*- and *y*-polarized electronic transitions, corresponding to a non-degenerate LUMO with a substantial energy gap between the LUMO and LUMO+1.[31-33] Examination of the phosphorescence emission and $T_1 \rightarrow T_n$ absorption data in Table 2 shows that in contrast to the fluorescent excited states of these species, the energies of the phosphorescent excited states are all very similar for these highly conjugated porphyrin arrays, regardless of the nature of the porphyrin-to-porphyrin connectivity. Equally interesting is the little variance among the $T_n - T_1$ energy separations in compounds **8**−**15**; all of these transitions are on average 2000 cm^{-1} to the red of the $T_n - T_1$ gap observed for ZnTPP. These results suggest that the nature of the photoactivated triplet state is similar in all these species and is consistent with the picture that emerges from the low-temperature EPR spectroscopy: namely, that the lowest energy photoactivated triplet corresponds to first approximation to an excited state essentially localized on a single (porphinato)zinc unit in these arrays. Future studies with respect to the triplet photophysics of these conjugated porphyrin arrays will focus on examining the transient optical spectra in the low energy visible and near infrared regions of the spectrum to ascertain whether there exists any spectral signatures that depend intimately on the porphyrin-to-porphyrin linkage topology.

Conclusion

All of the ethyne- and butadiyne-bridged (porphinato)zinc arrays along with their ethyne- and butadiyne-elaborated monomeric porphyrinic building blocks exhibit electron spin polarization patterns verifying that intersystem crossing from the first excited singlet state occurs predominantly through the $|T_z\rangle$ spin state sublevel. For the monomeric (porphinato)zinc species **2**, **3**, **4**, **6**, and **7**, the major effect of ethynyl or butadiynyl elaboration of the porphyrin periphery appears to be a reduction in the photoactivated triplet state symmetry, which render these states stable with respect to Jahn−Teller distortion. The triplet excited state of ethyne- and butadiyne-bridged (porphinato)zinc arrays **8**−**15** is essentially localized upon a single chromophore in the assembly, as indicated by both the magnitude of the EPR *D* values and the room temperature $T_1 \rightarrow T_n$ absorption spectra. This lack of global excitation delocalization for the photoactivated triplet state of these (porphinato)zinc arrays stands in marked contrast to their photoexcited singlet states which evince highly delocalized electronic distributions, the extent and nature of which depend intimately on the mode of porphyrin-to-porphyrin connectivity.[31-33]

Perhaps the most striking aspect of this study is how the chromophore-to-chromophore linkage topology impacts both spin distribution and spin alignment in the low-temperature photoactivated triplet states of conjugated (porphinato)zinc arrays **8**−**15**; these observations are summarized in Figure 11. Class I arrays feature β-to-β ethyne and butadiyne linkages and

(72) (a) Walters, V. A.; de Paula, J. C.; Jackson, B.; Nataitis, C.; Hall, K.; Lind, J.; Cardozo, K.; Chandran, K.; Raible, D.; Phillips, C. M. *J. Phys. Chem.* **1995**, *99*, 1166−1171. (b) Rodriquez, J.; Kirmaier, C.; Holten, D. *J. Am. Chem. Soc.* **1989**, *111*, 6500−6506. (c) Weiss, C.; Kobayashi, H.; Gouterman, M. *J. Mol Spectrosc.* **1965**, *16*, 415−450.

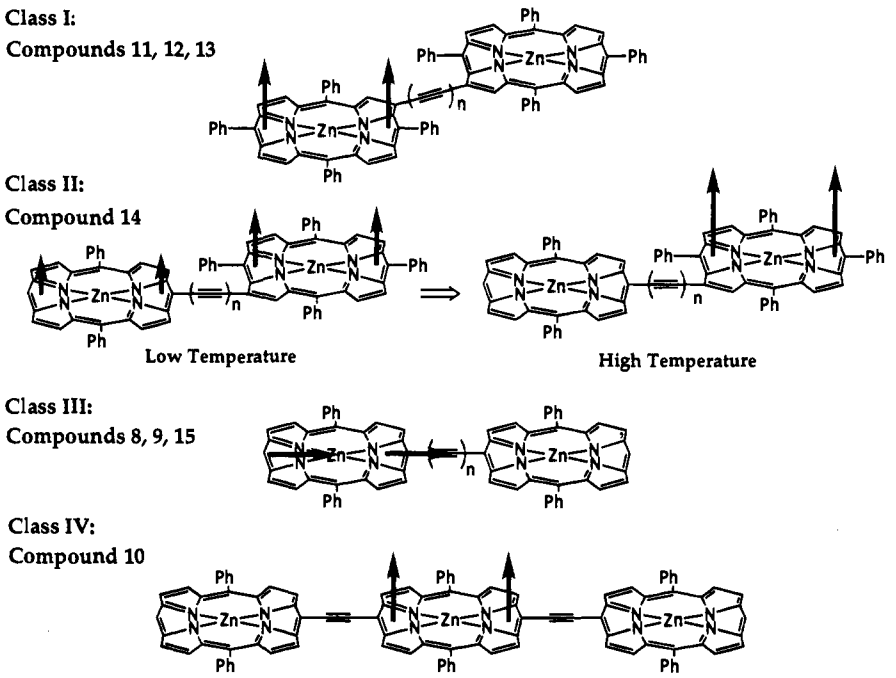

Figure 11. Schematic drawing illustrating both spin distribution and spin alignment for the low temperature photoactivated triplet states of the conjugated (porphinato)zinc arrays examined in this study.

exhibit spin localization on a single ZnTPP unit with spin polarization along the z direction, perpendicular to the porphyrin plane. The driving force for spin localization for these compounds likely derives from the anisotropic nature of the low temperature matrix about each of the (porphinato)zinc units of the array. Only the *meso*-to-β ethyne-bridged dimer **14** belongs to class II; it is exceptional in that at low temperature it exhibits z-polarized triplets partially localized on both the ZnDPP and ZnTPP components of the array. As the temperature is increased from 4 K, the spin becomes localized on the 2-ethynyl-ZnTPP portion of the molecule. This behavior derives from temperature-dependent electronic coupling that has its genesis with the mutually orthogonal relationship of the (porphinato)zinc moieties of the dimeric array; at low temperature the orthogonal π systems do not permit effective electronic communication between the chromophores. As the temperature increases, librational motions of the chromophores about the ethyne bridge facilitate enhanced electronic coupling which eventually results in spin localization on the ZnTPP portion of the monomer, which possesses the lowest energy triplet state. As such, molecule **14** constitutes a rare if not unique example of a molecular system in which electronic coupling is thermally activated within a low-temperature glassy matrix. Compounds **8**, **9**, and **15** define the class III (porphinato)zinc arrays; the large electronic coupling exhibited between the constituent ZnDPP chromophores of the symmetrical dimers **8** and **9**, as well as between the ZnDPP and ZnTPP units of the *meso*-to-β butadiynyl-bridged bis[(porphinato)zinc] complex (**15**), results in an oblate-to-prolate spin transition. The direction of the largest dipolar interaction is no longer along the z direction but lies in the porphyrin plane polarized along the molecular dimension of highest conjugation. In compounds **8** and **9**, for example, this results in a head-to-tail alignment of the spin density localized largely on a single ZnDPP unit. For such an electronic distribution, the interelectron distance must be enhanced for arrays within class III relative to those belonging to classes I, II, and IV, as well as with respect to monomeric porphyrins **2**, **3**, **4**, **6**, and **7** to account for the magnitudes of the observed D values for bis[(porphinato)zinc] complexes **8**, **9**, and **15**. Furthermore, the increase in the magnitude of D in **9** relative to **8** suggests that it may be possible to amplify the interelectron separation distance, simply by fabricating oligomers or polymers that feature the modes of chromophore-to-chromophore connectivity defined within this class of conjugated bis[(porphinato)zinc] species. Class IV arrays are related to those belonging to class I in that they exhibit spin localization on a single (porphinato)zinc unit with direction of the largest dipolar interaction polarized along z. Molecules within class IV contrast those within class I: for example, the spin localization observed for array **10** must derive primarily from the inherent electronic asymmetry of the constituent chromophoric building blocks composing the supermolecule and not glassy matrix anisotropy about the (porphinato)zinc units.

Finally, these highly conjugated dimeric and trimeric (porphinato)zinc complexes are remarkable in maintaining spin polarization up to the highest measurable temperature. One can speculate that such compounds and their higher order arrays may have very long spin diffusion lengths and could consequently be used for molecular-based optoelectronic spin transistors.[73]

Acknowledgment. This work was done in partial fulfillment of the requirements of the Ph.D. degree by P.J.A. and V.S.-Y.L. It was supported by National Institutes of Health Grant PO1 GM48130. The authors wish to thank Prof. Hans van Willigen and Dr. John S. Leigh for helpful discussions and Dr. Jonathan Casper of DuPont Central Research for his assistance with the phosphorescence measurements. M.J.T. is extremely grateful to the Searle Scholars Program (Chicago Community Trust), the Arnold and Mabel Beckman Foundation, E. I. du Pont de Nemours, and the National Science Foundation for Young Investigator Awards, as well as to the Alfred P. Sloan Foundation for a research fellowship.

JA952170V

(73) Prinz, G. A. *Phys. Today* **1995**, *48*, 58–63.